Dissertation

submitted to the
Combined Faculties for the Natural Sciences and for Mathematics
of the Ruperto-Carola University of Heidelberg, Germany

for the degree of
Doctor of Natural Sciences

Put forward by

Stewart "Mac" Biedeman Mein IV
Born in Princeton, New Jersey, USA

Oral examination: February 7th, 2020

FRoG: a fast robust analytical dose engine on GPU for p, ^{4}He, ^{12}C and ^{16}O particle therapy

Referees: Prof. Dr. Dr. Jürgen Debus

Prof. Dr. Oliver Jäkel

"To cease to think creatively is to cease to live."

— Benjamin Franklin

FRoG: a fast robust analytical dose engine on GPU for p, ^{4}He, ^{12}C and ^{16}O particle therapy

Radiotherapy with protons and heavier ions landmarks a novel era in the field of high-precision cancer therapy. To identify patients most benefiting from this technologically demanding therapy, fast assessment of comparative treatment plans utilizing different ion species is urgently needed. Moreover, to overcome uncertainties of actual in-vivo physical dose distribution and biological effects elicited by different radiation qualities, development of a reliable high-throughput algorithm is required. To this end, we engineered a unique graphics processing unit (GPU) based software architecture allowing rapid and robust dose calculation. Fast dose Recalculation on GPU (FRoG) currently operates with four particle beams, i.e., raster-scanning proton, helium, carbon and oxygen ions. Designed to perform fast and accurate calculations for both physical and biophysical quantities, FRoG operates an advanced analytical pencil beam algorithm using parallelized procedures on a GPU. Clinicians and medical physicists can assess both dose and dose-averaged linear energy transfer (LET) distributions for proton therapy (and in turn effective dose by applying variable RBE schemes) to further scrutinize plans for acceptance or potential re-planning purposes within minutes. In addition, various biological model predictions are readily accessible for heavy ion therapy, such as the local effect model (LEM) and microdosimetric kinetic model (MKM). FRoG has been extensively benchmarked against gold standard Monte Carlo simulations and experimental data. Evaluating against commercial treatment planning systems demonstrates the strength of FRoG in better predicting dose distributions in complex clinical settings. In preparation for the upcoming translation of novel ions, case-/disease-specific ion-beam selection and advanced multi-particle treatment modalities at the Heidelberg Ion-beam Therapy Center (HIT), we quantified the accuracy limits in particle therapy treatment planning under complex heterogeneous conditions for the four ions (p, ^{4}He, ^{12}C, ^{16}O) for various dose engines, both analytical algorithms and Monte Carlo code. Devised in-house, FRoG landmarks the first GPU-based treatment planning system (non-commercial) for raster-scanning ^{4}He ion beams, with an official treatment program set for early 2020. Since its inception, FRoG has been installed and is currently in operation clinically at four centers across Europe: HIT (Heidelberg, Germany), CNAO (Pavia, Italy) , Aarhus (Denmark) and the Normandy Proton Therapy Center (Caen, France). Here, the development and validation of FRoG as well as clinical investigations and advanced topics in particle therapy dose calculation are covered. The thesis is presented in cumulative format and comprises four peer-reviewed publications.

FRoG: eine schnelle robuste analytische Dosis-Engine für die GPU mit p, ^{4}He, ^{12}C und ^{16}O Partikeltherapie

Strahlentherapie mit Protonen und schweren geladenen Teilchen hat eine neue Ära der Krebstherapie eingeleitet. Um Patienten, die von dieser technisch anspruchsvollen Methode am meisten profitieren würden, zu identifizieren, ist ein schneller Vergleich von Bestrahlungsplänen mit unterschiedlichen Teilchenarten unabdingbar. Aus diesem Grund wurde ein neuartiges, Graphikkarten-basiertes Computerprogramm geschrieben, welches schnelle und robuste Dosisberechnung ermöglicht. Fast dose Recalculation on GPU"(engl. für SSchnelle Dosis-Nachberechnung mit Graphikkartenprozessoren"), FRoG, unterstützt Dosisberechnungen für Protonen-, Heliumionen-, Kohlenstoffionen- und Sauerstoffionenbestrahlung. FRoG wurde mit einen hochentwickelten, analytischen Pencil-Beam-Algorithmus entwickelt, der die Parallelität von Grafikkartenberechnung ausnutzt. Dies erlaubt schnelle und präzise (bio-) physikalische Dosisberechnung. Mediziner und Medizinphysiker erlangen mit FRoG Zugang zu Dosis-gewichtetem linearen Energie Übertrag von Protonen und daraus folgend auch zu effektiver Strahlendosis durch Anwendung verschiedener Biophysischer Modelle für RBE. Sie können damit innerhalb Minuten entscheiden, ob ein Bestrahlungsplan akzeptabel ist oder neu geplant werden muss. Darüber hinaus sind auch verschiedene biophysikalische Modelle für Teilchenbestrahlung mit schweren Ionen, wie LEM oder MKM, integriert. FRoG wurde ausführlich gegen Monte Carlo Simulationen, die als Maßstab in der Teilchentherapie gelten, und experimentelle Messungen verifiziert. Der Vergleich zu einem klinisch verwendeten Bestrahlungsplanungssystem zeigte außerdem, dass FRoG besonders in komplexen klinischen Szenarien Strahlendosis genauer vorhersagen konnte. In Vorbereitung auf die bevorstehende Einführung von neuen Teilchen, Fall und Krankheitsspezifische Bestrahlungsplanung oder komplexen Mehr-Ionen-Plänen für die Tumorbestrahlung für die Teilchenbestrahlung am Heidelberg Ionenstrahl-Therapiezentrum (HIT) wurde die Genauigkeitsgrenze in der Bestrahlungsplanung unter komplexen und heterogenen Bedingungen für die vier Teilchenarten analysiert. Dabei wurden sowohl analytische Programme, als auch Monte Carlo Simulationen verwendet. FRoG ist das erste GPU basierte (nicht kommerzielle) Bestrahlungsplanungssystem für ^{4}He Heliumionen im Rasterscan-Verfahren, mit denen ab 2020 behandelt wird, und wurde vor Ort für das HIT entwickelt. In diesem Zusammenhang wurden auch die biophysikalischen Aspekte von Heliumionen mit in-vitro Clonogenic-Assays, Monte Carlo Simulationen mit existierenden RBE Modellen untersucht, und FRoG für biologische Dosisberechnung mit Heliumionen validiert. Seit seiner Entwicklung ist FRoG an vier Standorten innerhalb Europa installiert worden: am HIT (Heidelberg, Germany), am CNAO (Pavia, Italy), in Aarhus (Dänemark) und am Normandy Proton Therapy Center (Caen, France). Hier werden sowohl die Entwicklung und Validierung von FRoG, als auch klinische Untersuchungen und erweiterte Themen in der Dosisberechnung von Teilchenstrahlen vorangetrieben. Diese Thesis wird im kumulativen Format vorgelegt und beinhaltet vier von unabhängigen Experten begutachtete Publikationen.

Contents

List of Publications

---

5 published, 1 in press

i. **Mein S**, Choi K, Kopp B, Tessonnier T, Bauer J, Alfredo F, Haberer T, Debus J, Abdollahi A and Mairani. Fast robust dose calculation on GPU for high-precision ^{1}H, ^{4}He, ^{12}C and ^{16}O ion therapy: the FRoG platform. *Sci. Rep.*, 2018.

ii. Choi K, **Mein S**,, Kopp B, Magro G, Molinelli S, Ciocca M and Mairani A. FRoG—A New Calculation Engine for Clinical Investigations with Proton and Carbon Ion Beams at CNAO. *Cancers*, 2018.

iii. **Mein S**, Kopp B, Tessonnier T, Ackermann B, Ecker S, Bauer J, Choi K, Aricò G, Ferrari A, Haberer T, Debus J, Abdollahi A and Mairani A. Dosimetric validation of Monte Carlo and analytical dose engines with raster-scanning ^{1}H, ^{4}He, ^{12}C and ^{16}O ion-beams using an anthropomorphic phantom. *Phys. Med.*, 2019.

iv. **Mein S**, Dokic I, Klein C, Tessonnier T, Böhlen T T, Magro G, Bauer J, Ferrari A, Parodi K, Haberer T, Debus J, Abdollahi A and Mairani A 2019a Biophysical modeling and experimental validation of relative biological effectiveness (RBE) for 4He ion beam therapy. *Radiat. Oncol.*, 2019.

v. Klein C, Dokic I, Mairani A, **Mein S**, Brons S, Häring P, Zimmerman A, Zenke F, Blaukat A, Debus J, Abdollahi A. Overcoming hypoxia-induced tumor radioresistance in non-small cell lung cancer by targeting DNA-dependent protein kinase in combination with carbon ion irradiation. *Radiat. Oncol.*, 2017.

vi. Kopp B, **Mein S**, Dokic I, Harrabi S, Böhlen T T, Haberer T, Debus J, Abdollahi A, Mairani A. Development and validaiton of single field multi-ion therapy treatments. *International Journal of Radiation Oncology*Biology*Physics*, 2019 (in press).

Conference contributions

S. Mein, B. Kopp, I. Dokic, S. Harrabi, T.T. Böhlen, T. Haberer. J. Debus, A. Abdollahi, A. Mairani. Combined Ion-beam Constant RBE (CICR): development and validation of a novel particle therapy modality. ENLIGHT Annual Meeting, Caen, France, 2019.

F. Faller, **S. Mein**, A. Mairani. Dosimetric validation of spectral CT-based stopping power prediction for proton beams using an anthropomorphic head phantom. ICCR-MCMA, Montreal, Canada, 2019.

S. Mein, T. Tessonnier, B. Kopp, A. Mairani. Integration and application of an independent GPU-based dose engine (FRoG) at the Normandy Proton Therapy Center. PTCOG 58, Manchester, UK, 2019.

B. Kopp, **S. Mein**, A Mairani. Multi ion biological and physical dose optimization with the FRoG framework. PTCOG 58, Manchester, UK, 2019.

B. Kopp, **S. Mein**, A Mairani. Implementation and commissioning of the FRoG framework at the DCPT. PTCOG 58, Manchester, UK, 2019.

A. Mairani, K. Choi, B. Kopp, **S. Mein**. FRoG: a platform for rapid and robust clinical dose calculations in hadron therapy. PTCOG 58, Manchester, UK, 2019.

B. Kopp, **S. Mein**, K. Choi, T. Haberer, J. Debus, A. Abdollahi, A. Mairani. Fast dose Recalculation on GPU at the Heidelberg Ion-beam Therapy center. ICCR-MCMA, Montreal, Canada, 2019.

K. Choi, **S. Mein**, B. Kopp, A Mairani. New modalities for FRoG: Sandbox strategy applied to pelvic cancer patients treated with carbon ion therapy at CNAO. PTCOG 57, Cincinnati, USA, 2018.

K. Choi, **S. Mein**, B. Kopp, A Mairani. FROG - new calculation engine for physical and biological dose investigations at CNAO. PTCOG 57, Tokyo, Japan, 2017.

T. Tessonnier, **S. Mein**, B. Kopp, K. Choi, T Haberer, J Debus, A Abdollahi, A Mairani. Evaluation of lateral density heterogeneity handling in a novel GPU-based pencil beam algorithm. ESTRO37, Barcelona, Spain, 2017.

S. Mein, T. Tessonnier, B. Kopp, K. Choi, T Haberer, J Debus, A Abdollahi, A Mairani. FROG: a novel GPU-based approach to the pencil beam algorithm for particle therapy. Evaluation of lateral density heterogeneity handling in a novel GPU-based pencil beam algorithm. ESTRO37, Barcelona, Spain, 2017.

S. Mein, T. Tessonnier, C Klein, I Dokic, K Parodi, T Haberer, J Debus, A Abdollahi, A Mairani. Monte Carlo calculation of RBE and in vitro validation for helium ion-beam therapy. MCMA, Naples, Italy, 2017.

C Klein , I Dokic, A Mairani, **S. Mein**, S Brons, J Debus, A Abdollahi. Overcoming hypoxia-induced radioresistance by targeting the DNA damage response in combination with proton, helium-, carbon- and oxygen ion beams, Wolfsberg Conference, Germany, 2017.

S. Mein, T. Tessonnier, C Klein, I Dokic, K Parodi, T Haberer, J Debus, A Abdollahi, A Mairani. Initial experimental investigation of RBE prediction in 4He ion-beam therapy. PTCOG56, Tokyo, Japan, 2017.

List of Acronyms

BAMS	Beam applications and monitoring system
BP	Bragg peak
CERN	European center for nuclear research
CNAO	National Centre for Oncological Hadrontherapy
CPU	Central processing unit
CT	computed tomography
CTV	Beam applications and monitoring system
DFO	Distal fall-off
DG	Double Gaussian
DKFZ	German Cancer Research Center
DNA	Deoxyribonucleic acid
GPU	Graphics processing unit
DSB	Double strand break
DVH	Dose volume histogram
FRoG	Fast Robust dose calculation on GPU
FWHM	Full-width at half-maximum
GSI	Helmholtzzentrum für Schwerionenforschung
Gy	Unit (Gray) for absorbed dose
GyRBE	Unit for RBE-weighted dose / biological dose
HIT	Heidelberg Ion-beam Therapy Center
HU	Hounsfield units

IC Ionization chamber

IDD Integral depth dose

IMPT Intensity-modulated particle therapy

IMRT Intensity-modulated radiotherapy

LBL Lawrence Berkeley Laboratory

LEM Local effect model

LIBC Library of ion beam characteristics

LET linear energy transfer

LQ Linear quadratic

MC Monte Carlo

MCTP Monte Carlo Treatment Planning platform

MKM Microdosimetric kinetic model

MWPC Multiple wires proportional chamber

NIRS National Institute of Radiological Sciences

NTCP Normal tissue complication probability

OAR Organ at risk

OER Oxygen enhancement ratio

PTV Planning target volume

RBE Relative biological effectiveness

RiFi Ripple filter

SG Single Gaussian

SOBP Spread-out Bragg peak

SSB Single strand break

TCP Tumor control probability

TG Triple Gaussian

TPS Treatment planning system

WEPL Water equivalent path length

1 Introduction

1.1 Motivation

Radiotherapy (RT) is a cornerstone in the treatment of cancer. Nearly two-thirds of all cancer patients receive some form of radiotherapy. Most of these patients undergo either photon- and/or electron-based therapies due to their longstanding use, accessibility and cost (Baskar et al. 2012), including brachytherapy or external beam radiotherapy (Daniel Bourland 2011). Particle therapy, on the other hand, is on the rise, offering treatment options for patients with unresectable, inoperable and radio-resistant tumors, as well as sensitive patients e.g. in pediatrics where minimization of radiation dose to healthy tissues is critical.

The concept of particle therapy was first developed at Harvard University by a group of scientists led by Robert Wilson in 1946 (Wilson 1946, Endo 2018) and subsequently adopted years later by the Lawrence Berkeley Laboratory (LBL), where years of experimentation to characterize both physical and biological properties of various ion beams and the first proton therapy patient treatments in 1954 took place (Lawrence et al. 1963, Lawrence et al. 1965, Lyman and Howard 1977). Technological advances in the last decade have made these cutting-edge modalities more accessible to the general public. Through application of state-of-the-art delivery systems, such as three-dimensional intensity-controlled raster scanning, patients with aggressive radio-resistant disease can be effectively treated. Currently, the leading modalities in hadrontherapy use protons and carbon ion beams (Durante et al. 2017).

Radiotherapy's mechanism lay predominately in damaging deoxyribonucleic acid (DNA) and fundamental structures of tumorous cells by the process of ionization, inducing either direct or indirect damage (Fig. 1.1). Single strand break (SSB), double strand break (DSB) production, or even more more complex clustered strand breaks, can activate various cellular responses, leading to repair, disrepair or programmed cell-death (Hall et al. 1988, Goodhead 1994, Goodhead 2006). Cancer is inherently an invasive and aggressive disease with high order of dysfunction, resistance to treatment and fast proliferation. Fast proliferating tissues are most

susceptible to radiation-induced death due to their inability to properly repair DNA damage. This is a key factor in the efficacy of radiotherapy.

The first localization of tumor cells is referred to as the primary cancer and can eventually progresses by invading (metastasize) other parts of the body. The traditional approach to treating cancer involves surgery, radiotherapy, chemotherapy or a combination of these treatments (Durante and Loeffler 2010). Experimental therapies such as immunotherapy and adjuvant treatments also show promise to improve clinical outcome (Oiseth and Aziz 2017, Lee et al. 2018).

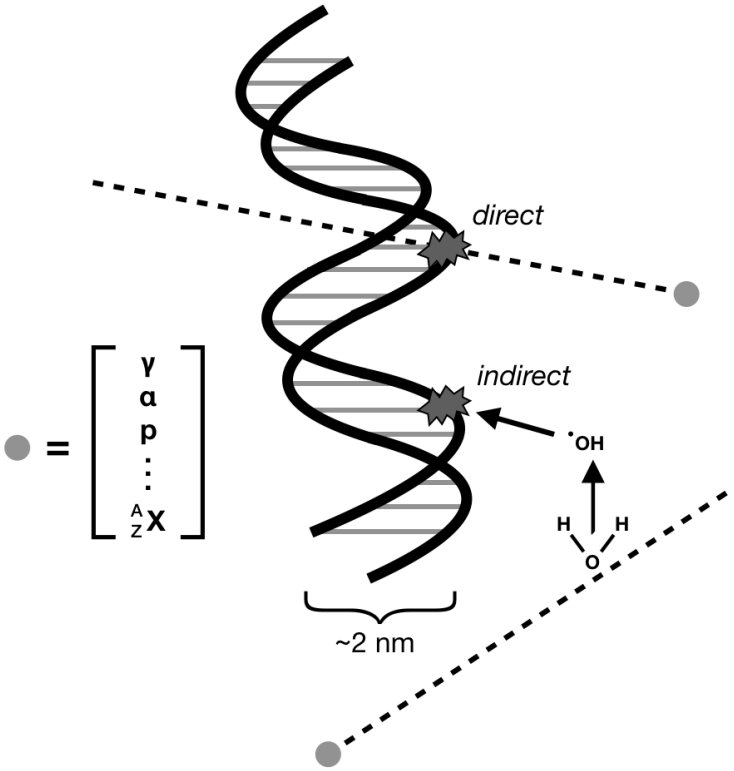

Figure 1.1 – Indirect versus direct radiation-induced DNA damage.

For all curative cancer treatments (as opposed to palliative), the main goal is eradication of malignant cells while sparing healthy tissues and critical organs. In radiotherapy, this balance is crucial to assure tumor control and decrease risk of radiation induced effects and secondary cancer in the normal tissue. Hence, target conformity is a key clinical concept during treatment planning and delivery, aiming to increase dose to the tumor while reducing dose to normal healthy tissues. So, the physical quantity dose (D) for a particles (dN) traversing and infinitesimal cylinder of cross sectional area dA and thickness d_x is defined as

$$D \equiv \frac{\text{energy}}{\text{mass}} = \frac{-(dE/dx) \times dx \times dN}{\rho \times dA \times dx} \tag{1.1}$$

or more simply

$$D \equiv \Phi \frac{\mathrm{S}}{\rho} \tag{1.2}$$

In short, dose equals fluence (Φ), which is the time-integrated particle flux, times mass stopping power (S), which is the retarding force acting on the charged particle radiation (ρ) (Jennings 1994). Absorbed dose is expressed in the unit of the Gray ($Gy = J/kg$).

Theoretically, particle beams have the greatest potential for normal tissue sparing compared to conventional modalities like photons and electrons (linear attenuation), since the characteristics of particle beam dose deposition provide more advantageous physical distributions and biological effects (Schardt et al. 2010). Figure 1.2 depicts relative dose deposition curves for various radiation qualities available at the Heidelberg University Clinic, for photon (γ) and particles (protons (^{1}H), helium (^{4}He) ions, carbon (^{12}C) ions and oxygen (^{16}O) ions). The Bragg peak (BP) refers to the entire depth dose distribution measured for a specific beam energy of particles and is this characteristic curve in particle therapy. The integral depth dose for each BP as a function of depth is commonly measured in a water tank for each treatment room during commissioning. The depth of BP's maximum can be manipulated as a function of energy. To uniformly deliver a specified prescription dose in a target, a superposition of those BP's varying in energy, position and spot-size form the spread out Bragg Peak (SOBP).

A trade-off then has to be considered to satisfy this balance between an effective treatment and avoiding/decreasing complications and risk of secondary cancer in the normal tissue. In order to achieve this goal, conventional radiotherapy techniques using high energy photons evolved to provide a more conformal dose delivery to the tumor, with technologies such as the multi-leaf collimator (MLC) (Boyer et al. 2001). The degree of conformity using collimation is limited, however, due to the primary physical interaction mechanisms for photons with energy in the therapeutic range (coherent scattering, incoherent scattering, etc.), yielding a significant lateral penumbra. Additionally, due to linear attenuation, photon treatments often use several beams with different angles/entry points to increase dose to deep-seated tumors. Due to their more favorable physical properties, ion beams are seen as an attractive alternative to photons. Currently, all treatment prescriptions for both photon- and particle-based therapies are constructed from decades of clinical experience with photon treatments. Tumor control probability (TCP) and normal tissue complication probability (NTCP) models help guide the clinician in assigning success rates to specific treatment regimens while balancing risk of damaging healthy tissues (Baumann and Petersen 2005). In practice, the dose-volume histogram (DVH) is a vital computational tool to evaluate and visually quantify the quality of a treatment plan's target (tumor) dose coverage and the degree of healthy tissue sparing. of Quantitative Analyses of Normal Tissue Effects in the Clinic (QUANTEC), for example, provides insight into the current clinical estimates for

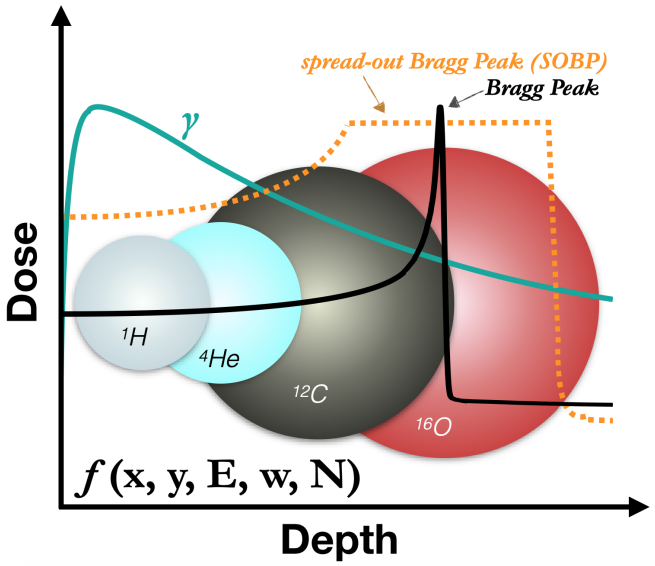

Figure 1.2 – Qualitative comparison of depth-dose profiles for different radiation qualities: photons (γ), protons (^{1}H), helium (^{4}He) ions, carbon (^{12}C) ions and oxygen (^{16}O) ions. Generalized Bragg peak (black arrow) and spread out Bragg peak (orange arrow) are plotted, demonstrating unique physical characteristics when using particle beams as opposed to conventional photon based radiation, where maximal dose deposition occurs at the entrance and diminishes as a function of depth. To reach prescription doses in deep-seated tumors, photon treatments will use multiple beam angles to avoid delivering high doses to normal tissues within the entrance channel, while particle treatments may require only a single field and improve normal tissue sparing with reduced dose and volume irradiated compared to photons. Particle therapy modalities include passive scattering and active (raster) scanning. The latter involves "painting" dose within a target through a superposition of beam-spots with a particular size (w) and fluence (N) to create volume of delivered dose, generated by cycling through energy slices (E) for BP depth positioning, and altering lateral position of each spot (x,y) via steering magnets.

healthy tissue constraints and the predictive power of RT-related toxicity (Bentzen et al. 2010).

1.2 Physics of charged particles

The basis of the physics of particle radiation with matter begins with the Bethe-Bloch equation, first derived in 1933, to describe the energy loss as the mass stopping power in an elementary material Z with atomic number A:

$$-\left\langle \frac{dE}{dx} \right\rangle = Kz^2 \frac{Z}{A} \frac{1}{\beta^2} \left[\frac{1}{2} \ln \frac{2m_e c^2 \beta^2 \gamma^2 T_{\max}}{I^2} - \beta^2 - \frac{\delta(\beta\gamma)}{2} \right] \tag{1.3}$$

where K and T_{max} which represent constants and the maximum energy transfer in single collision, respectively, are described as

$$\mathrm{K} = 4\pi \mathrm{N_A} \mathrm{r_e^2} \mathrm{m_e c^2} = 0.307 \mathrm{MeV g^{-1} cm^2}$$

$$\mathrm{T_{max}} = 2\mathrm{m_e C^2} \beta^2 \gamma^2 / \left(1 + 2\gamma \mathrm{m_e/M} + (\mathrm{m_e/M})^2\right)$$

with z and M represent the charge and mass of incident particle. Z, A and I indicate the charge number, atomic mass and Mean excitation energy of medium. δ is a density correction for the transverse extension of electric field, $\beta = v/c$, Avogadro's number $N_a = 6.022 \times 10^{23}$, the rest energy of an electron $m_e c^2 \equiv 0.511$ MeV and the radius of an electron $r_e = e^2/4\pi\varepsilon_0 m_e C^2 = 2.8$fm. I, for the purposes of this work, can be used as an adjustable parameter of the theory during simulation.

The Bethe-Bloch equation is one fundamental description of physical phenomena in particle physics with both non-relativistic and relativistic solutions. By reducing terms and constants, one major take away is the energy loss dependence on mass A and charge Z of target nucleus approximated as

$$-\left\langle \frac{dE}{dx} \right\rangle \sim \frac{Z}{A} \tag{1.4}$$

which is also referred to at the stopping power (S). The mean projected (theoretical) range of an accelerated particle can be described as

$$R\left(E_{\text{initial}}\right) = \int_{E_{\text{minul}}}^{E_{\text{fratu}}} \left(\frac{1}{\rho}\frac{dE}{dx}\right)^{-1} dE = \int_{E_{\text{tral}}}^{E_{\text{math}}} \frac{dE}{S/\rho} \tag{1.5}$$

in units of g/cm^2.

Practically however, energy loss does not occur as a continuous process, but instead as a finite number of individual interactions. Therefore, energy loss can be considered a statistical phenomenon and consequently, leading to errors in predicted versus measured range for a single particle known as range straggling (or energy straggling). Practically, particle beam range is not measured for a single particle, but instead for a specific beam-line in several bunches or spills (on the order of tens of millions of particles) for improved statistics (Ondreka and Weinrich 2008). The net range of the particle beam is often quantified by a particular distance at which the fall-off dose reaches a certain percentage of the maximum BP, e.g. 80% ($\mathrm{R_{80}}$). As for stopping power, there are two main components to the stopping power — nuclear and electronic. Nuclear Stopping is more important for low energy heavy particles.

The main component is the electronic stopping which refers to projectile ion slowing down due to the inelastic collisions between bound electrons within the traversed medium.

As previously stated, one can consider the energy loss of particle radiation as a continuous process on a macroscopic scale. However, to most accurately model physical (and biological) effects of radiation, understanding the spatial distribution of energy loss and dosimetric characteristics of particle radiation on a microscopic scale is essential. The degree (or frequency) of energy loss within the radiation track structure is commonly referred to as the linear energy transfer (LET), defined as the energy deposited per unit distance along the track (i.e. $-dE/dx$) in units of keV per µm (Nikjoo et al.). Regarding its definition within the track structure, LET commonly considers the entire "infratrack" (centralized narrow track region approximately five interatomic distances radially) and a part of the "ultratrack" (outer shell caused by secondary electron induced excitations and ionizations which escape from the infratrack). For ion projectiles, the infratrack defines the region in which electrons of the traversed medium are attracted towards the positively charged particle. In terms of biology, an increased LET can produce more damage with increased complexity, which influences a cellular system's repair mechanisms, either due to the frequency or severity of damage. Dose-averaged LET (LET_d) values of clinical significance range from ~1 keV μm^{-1} to ~12 keV μm^{-1} for protons, ~4 keV μm^{-1} to ~50 keV μm^{-1} for helium ions, ~12 keV μm^{-1} to ~150 keV μm^{-1} for carbon ions and ~14 keV μm^{-1} to ~180 keV μm^{-1} for oxygen ions. Biological repercussions of radiation induced damage are briefly introduced in the following section.

1.3 Radiobiology of charged particles

For an equivalent local energy deposition (i.e. dose), particle beams are more effective than photons. To describe radiation induced death in a cell population, one can describe the cell survival (S), traditionally described as a linear-quadratic (LQ) with

$$S = \exp\left(\alpha D + \beta D^2\right) \tag{1.6}$$

where α and β represent the linear and quadratic coefficients, respectively, as a function of physical dose (D). The ratio of the linear and quadratic coefficients, $(\alpha/\beta)_x$), is often referred to as a description for the sensitivity of the cell line when exposed to photon radiation (x). Since a lower dose of particle radiation is required to produce the same biological effect when using photon radiation, we define the relative biological effectiveness (RBE) where

$$RBE[endpoint] = \frac{D_x}{D_z} \tag{1.7}$$

where RBE represents the iso-effective dose ratio between a particle radiation (D_z) and a reference radiation (D_x) and is modeled as a function of various endpoints. RBE is known to vary with tissue type ($(\alpha/\beta)_x$), dose (D_z) and LET; however these relations are complex and many recent efforts aim to devolve it's multi-dimensional dependencies (Fig. 1.3). In general, RBE increases with decreasing dose and $\alpha/\beta)_x$, while RBE increases with increasing LET until a certain maximum where a saturation effect occurs. LET is, however, a crude descriptor for the complex track damage of particle radiation and has been demonstrated as a poor indicator for RBE (even for protons) (Giovannini et al. 2016). In addition, the relationship of LET and RBE is particle species dependent, i.e. RBE for 12 keV µm^{-1} protons does equate 12 keV µm^{-1} carbon ions. Consideration of a mixed radiation field (i.e. the energy and particle species spectra) is therefore required for appropriate modeling of RBE for heavier ions.

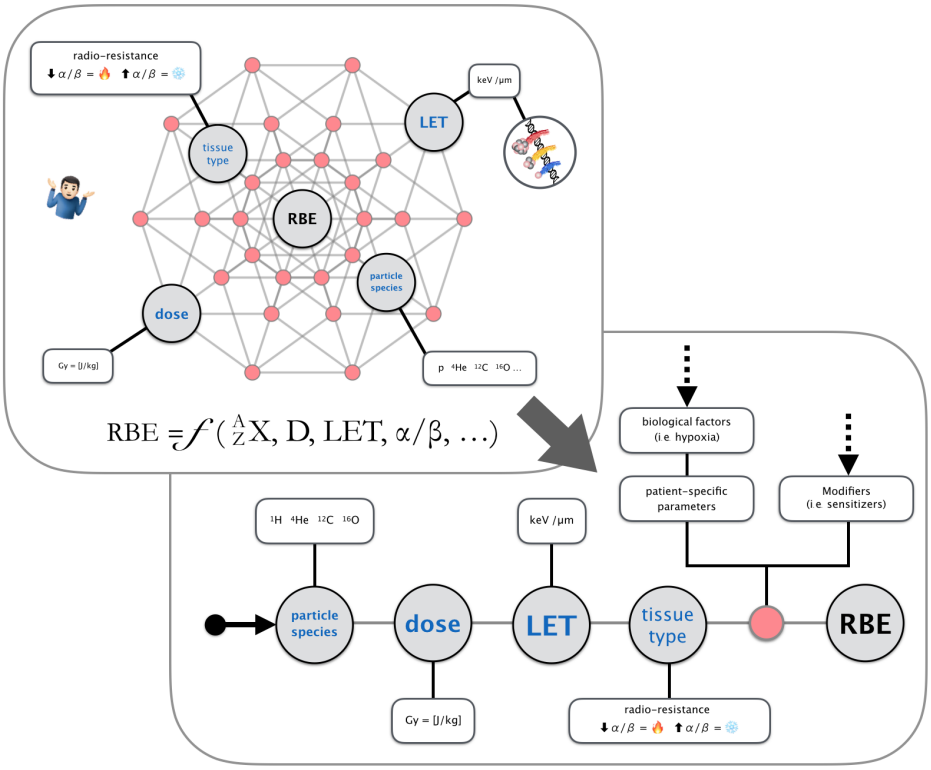

Figure 1.3 – "Understanding RBE." RBE is a complex quantity with both known and unknown endpoints. Traditionally, particle species, dose, tissue type and LET are the main dependencies. The ongoing classification and modeling of RBE within the field aims to unravel these main dependencies, as well as incorporate characteristics of the cellular environment, genomic factors and other patient-specific parameters.

From a practical standpoint, the RBE is a useful quantity for translating fractionation scheme, site-specific prescription doses, and dose constraints to critical structures from the photon world, since, in comparison to photons, substantially fewer patients have been treated with particle beams. From here, biological (or effective) dose is straightforward:

$$D_{RBE} = RBE \times D \tag{1.8}$$

To begin modeling the biological effectiveness of ion beams within the LQ framework, we can determine a dependency of RBE on the photon and particle radiation LQ-parameters. Considering that an absorbed dose D of particle radiation (D) and a photon dose (D_x) are iso-effective if

$$\alpha \mathrm{D} + \beta \mathrm{D}^2 = \alpha_{\mathrm{x}} \mathrm{D}_{\mathrm{x}} + \beta_{\mathrm{x}} \mathrm{D}_{\mathrm{x}}^2 \tag{1.9}$$

Then, we define two ratios composed of linear and quadratic terms separately:

$$\mathrm{RBE}_{\alpha} \equiv \frac{\alpha}{\alpha_{\mathrm{ph}}} \tag{1.10}$$

$$\mathrm{R}_{\beta} \equiv \frac{\beta}{\beta_{\mathrm{ph}}} \tag{1.11}$$

Next using equations 10 and 11, equation 9 can be rewritten as follows:

$$RBE\left(\left(\frac{\alpha}{\beta}\right)_{\mathrm{ph}}, D_{\mathrm{ph}}, \mathrm{RBE}_{\alpha}, \mathrm{R}_{\beta}\right) = \frac{\left(\frac{\alpha}{\beta}\right)_{\mathrm{ph}} \mathrm{RBE}_{\alpha} + \sqrt{\left(\frac{\alpha}{\beta}\right)_{\mathrm{ph}}^2 \mathrm{RBE}_{\alpha}^2 + 4 D_{\mathrm{ph}} \left[\left(\frac{\alpha}{\beta}\right)_{\mathrm{ph}} + D_{\mathrm{ph}}\right] \mathrm{R}_{\beta}}}{2\left[\left(\frac{\alpha}{\beta}\right)_{\mathrm{ph}} + D_{\mathrm{ph}}\right]} \tag{1.12}$$

to better highlight the dependence of RBE on photon parameters $\alpha/\beta)_x$ and D_x, as well as particle beam parameters RBE_{α} and R_{β}. If one performs derivations as function of the particle radiation dose, RBE is defined as

$$RBE\left(\left(\frac{\alpha}{\beta}\right)_{\mathrm{ph}}, D, \mathrm{RBE}_{\alpha}, \mathrm{R}_{\beta}\right) = -\frac{1}{2D}\left(\frac{\alpha}{\beta}\right)_{\mathrm{ph}} + \frac{1}{D}\sqrt{\frac{1}{4}\left(\frac{\alpha}{\beta}\right)_{\mathrm{ph}}^2 + \mathrm{RBE}_{\alpha}\left(\frac{\alpha}{\beta}\right)_{\mathrm{ph}} D + \mathrm{R}_{\beta} D^2} \tag{1.13}$$

There are several approaches to modeling RBE with different expressions for RBE_α and R_β, however most rest on the LQ-framework from a biophysical or mechanistic standpoint, as well as phenomenological (or data-driven) for the lighter ions (p and ^{4}He). In terms of clinical applications, centers in Europe and parts of Asia (i.e. China) apply the local effect model version I (LEM-I), first developed in 1997, while Japanese centers, which initially handled dose-response with a linear–quadratic model (Kanai et al. 1999), currently apply the Microdosimetric Kinetic model (MKM) (Hawkins 1998, Hawkins 2003, Inaniwa et al. 2010). These models are both based on biophysical principles (considering various factors such as reference radiation dose–response, track structure, initial DNA damage, target sizes, etc.) yet have inherently different approaches to calculation.

For LEM, LQ-parameters (intrinsic α_z and β_z) and dose threshold (Dt) are the main inputs (for each particle from Z =1 to Z = 6) via the PT RBE Generator software by Siemens following previous reports, while for MKM, the saturation-corrected dose-mean specific energy (z^*_{1D}) for is computed with a specific radius of the domain (R_d) and the radius of the cell nucleus (R_n). Phenomenological approaches rely heavily on the (in vitro) data available in the literature for development tuning. Recent works collected and reviewed such models currently available for proton beams (Rorvik et al. 2018. These models are discussed in more detail in Chapter 2, *Publication D*.

1.4 The Heidelberg Ion-beam Therapy Center (HIT) and the Biophysics in Particle Therapy (BioPT) group

The Heidelberg Ion-beam Therapy Center (HIT) is a synchrotron-based clinical facility (as opposed to cyclotron-based accelerators commonly used by major vendors in proton therapy) with an active beam scanning (or raster-scanning) delivery system similar to the prototype at previously developed in decades prior during the pilot project GSI Helmholtz Centre for Heavy Ion Research (Darmstadt, Germany). The ion beams originate from sources which produce positively charged ions (p, ^{4}He, ^{12}C or ^{16}O). A linear accelerator (commonly referred to as a Linac) accelerates the ions to 10% the speed of light. Once the ions enter the synchrotron, they circulate several million times and are subsequently accelerated to 75% the speed of light. The ion beams are then led to the treatment rooms (2 × fixed-beam and 1 × heavy-ion gantry) and the path is optimally directed via steering magnets which can induce shift horizontal or vertical shifts (Haberer et al. 2004). Since its inception in 2009, over 5000 patients have been treated with either protons or carbon ions (Fig. 1.4).

The synchrotron can accelerate 255 discrete energies for protons, helium ions and carbon ions with a max range of 32 cm (205 discrete energies for oxygen ions with

a max range of 23 cm). Energies for the proton and helium ion beams reach up to 220 MeV/u and 430 MeV/u for carbon and oxygen ions. The current clinical modalities at HIT include protons or carbon ions, with plans to start up the world's first raster-scanning helium ion-beam therapy program within the next year.

The HIT clinic uses the SyngoPT® commercial TPS (Siemens, Erlangen, Germany) for treatment planning with protons and carbon ion beams. SyngoPT® was developed in collaboration with GSI and their in-house developed TPS, TRiP98 (Kramer and Scholz 2000, Krämer 2009). SyngoPT® allows calculation of physical and biological dose distributions using the LEM-I for RBE predictions of carbon ion beams (Scholz et al. 1997), while for protons, a constant RBE value of 1.1 is assumed the clinically accepted standard worldwide (Paganetti et al. 2002). The treatment planning systems (TPS) uses an analytical approach to dose calculation (in the case of SyngoPT®, a type of ray-casting called WEPL-to-POI). The TPS calls on a physical database (obtained either through experimental measurements or measurement-validated Monte Carlo simulations during facility start-up/commissioning) describing the integral depth-dose and lateral dose profiles as a function of depth. Commissioning of a new clinical TPS (RayStation, RaySearch, Stockholm, Sweden) is underway at HIT, capable of both MC simulation and analytical code calculations.

To fully exploit charged particle therapy (CPT) with the utmost precision, modelling and predicting biophysical processes elicited from particle beam interactions within the human body, must be performed on both macroscopic and microscopic scales. To this end, a newly formed research group, "Biophysics in Particle Therapy group (BioPT)", has been based at HIT and the Heidelberg University Hospital. As opposed to traditional research groups, BioPT serves as a direct link between clinical physicians and physicists to experimental techniques in radiotherapy. Additionally, BioPT aims to introduce advanced computational methods for CPT into clinical environments, improve the accuracy of the clinical treatment planning systems (TPS) used daily by clinicians, support the validation, commissioning and routine clinical use of the TPS against dosimetric and in vitro biological measurements, and develop both analytical and Monte Carlo simulation-based tools. A combination of these efforts with clinical investigations using large patient cohorts aims to link clinical outcome to physical, biological and clinical endpoints to utilize light and heavy ion therapy in more patient-specific treatment agendas.

1.5 Dose calculation in particle therapy

Dose calculation plays a pivotal role in the particle therapy treatment chain. In its earlier form, radiotherapy planning was conducted through a series of so-called "hand calculations" for each delivered beam using tabulated reference dose curves. While considering appropriate tuning and dosimetric correction factors (e.g. daily fluctuations in temperature, pressure, etc.), necessary machine output factors known

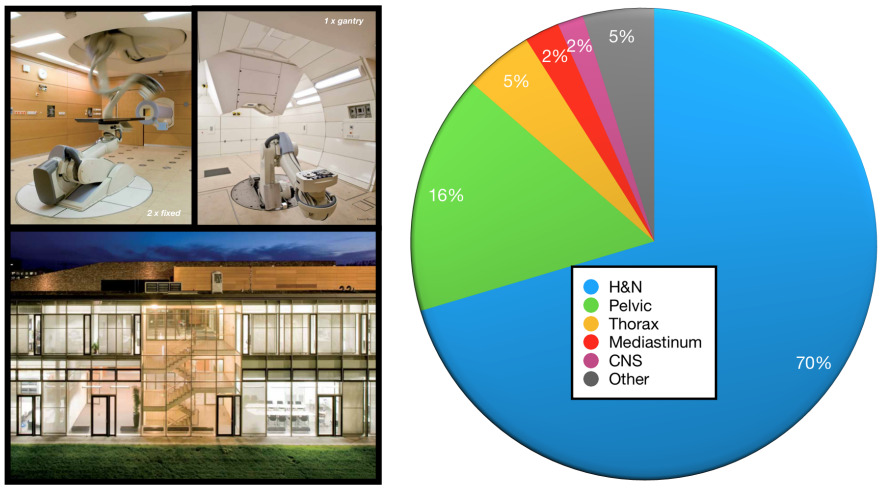

Figure 1.4 – The Heidelberg Ion-beam Therapy (HIT) facility (left), depicting the fixed-beam and gantry treatment rooms which deliver clinical beams (protons and carbon ions). A breakdown of clinical cases (right) is shown in the pie chart, with a majority of treatment cases in head and neck anatomical sites. Other represents treatments for liver, abdominal, extremities, pancreatic, etc.

as monitor units (MUs) or particle units (PUs) were estimated to reach prescription dose levels at a particular depth. Before the age of computers, these methods were understandably tedious and simplistic. Nowadays, dose computation with 3D modeling of the patient is routine, capable of generating sophisticated treatment plans e.g. intensity modulation via use of a multi-leaf collimator (mostly for photons) and active scanning pencil beam delivery methods.

The first requirement of a clinical TPS is that, compared to gold standard measurements and/or Monte Carlo simulations, its dose calculation engine must be accurate. The advantages BP in particle therapy is both advantageous feature (due to its inherent targeting) and potential risk, since the range is highly sensitive to uncertainty on the order of 2-3% (Paganetti 2012), especially in complex heterogeneous structure (like in a patient). Secondly, the TPS must be fast to meet the clinical needs during patient-specific treatment planning and quality assurance (QA). Attaining both accuracy and speed is a challenging feat but in spite of this, the two aspects of dose calculation have become even more critical as the demand for the particle therapy modalities increases and delivery techniques become more advanced (e.g. adaptive radiation therapy (ART) with on-board imaging). The clinical TPS is a powerful tool and is therefore be considered the workhorse in radiotherapy. The TPS is traditionally composed of an analytical algorithm (a set of functions or routines to approximate radiation physics) allowing for fast dose optimization, computation and assessment within the clinical time-frame.

Prior to treatment, each patient will undergo a series of imaging procedures using computed tomography (CT) systems and/or magnetic resonance imaging (MRI).

CT images provide electron density information, represented in diagnostic images as Hounsfield Units (HU), while MR images provide soft-tissue contrast. Both image modalities are vital to modern-day radiotherapy treatment planning. CT scans provide a 3-dimensional model of the patient to determine how the radiation transport will occur by correlating a particular image metric (conventionally HU) to stopping power ratio relative to water (SPR_w) in a scanner/protocol (scanner setting) specific look-up-table (LUT). This is particularly vital for particle therapy treatments, in that anatomic density will alter the finite range of the particle beam. As for MR images, physicians will use this enhanced soft-tissue visibility, not clearly distinguishable on CT images, to contour the tumor volume as well as healthy tissue and organs-at-risk (where dose minimization takes place during treatment plan optimization). After patient-specific information and modeling are available in the clinical TPS, patient treatment optimization is made possible.

Prior to facility start-up however, the clinical TPS will undergo a series of benchmark tests and validations to ensure the complex treatment planning procedures meet desired tolerances. In terms of dose prediction accuracy, Monte Carlo simulations are considered the gold standard but are often time-consuming. Here, a brief description of dose computation methods in particle therapy, Monte Carlo and analytical, will be introduced.

1.5.1 Monte Carlo codes

Computer simulations are useful tools during research and development. Modern-day Monte Carlo (MC) simulations, first theorized and applied during the Manhattan project in 1944 in the development of nuclear weapons, enable the mathematical representation of experimental conditions. In cases where experiments or measurements cannot be practically carried out, Monte Carlo systems offer a solution by incorporating physics models and information within a contained virtual environment, allowing research scientists to provide a "best-guess" (prediction) to nearly unanswerable questions (or immeasurable experiments). The accuracy of these answers depends on the proximity of the simulation (geometry and physics models) to reality. For example, in the upcoming manned missions to Mars, how much radiation will astronauts be exposed to on the Martian surface? What is the necessary amount of shielding to reduce risk of radiation-induced effects or diseases? Likewise, in regard to radiation oncology, what is the delivered dose to the patients? Unlike a physics experiments, we cannot directly probe or measure dose deposition within a patient during treatment to the degree that is desirable. Therefore, predictions, either via Monte Carlo or other means, are the main reference during treatment planning of verification.

Monte Carlo codes sample from stochastic distributions to simulate physics on a step-by-step basis by iterating the physics of each particle; their transport is based

on interaction probabilities (per unit distance) known as cross sections. In reality, interactions are discrete processes which include nuclear interactions, secondary particle production (including δ-electrons), and large angle Coulomb scattering.

In order to produce simulation resultants with an acceptable level of statistical strength in a typical radiation treatment, a large number of particle histories must be performed and therefore, are not only computationally intensive but also time-consuming. It is therefore clinically preferable to use simplified physics calculation codes on a daily basis.

In this work, Monte Carlo simulations are performed using FLUKA to verify a particular experiment or evaluate dose engine performance (Ferrari and others 2005, Böhlen et al. 2014, Battistoni et al. 2016). FLUKA is a general purpose tool and Monte Carlo code for calculations of particle transport and interactions with matter. Written in `FORTRAN77`, FLUKA was first developed in the 1960's (European Organization for Nuclear Research (CERN)) and is continually under-development today. The internal simulation framework known as FICTION is based on prior efforts which meticulously generated a simulation geometry/model of the HIT beam-line (Parodi et al. 2012, Bauer et al. 2014, Tessonnier et al. 2016). FLUKA and FICTION are particularly useful from both a clinical and research perspective, serving as the "gold standard" reference (in combination with measurements, when available) and verifying treatment plans calculated with analytical dose algorithms, like that of the standard clinical TPS.

1.5.2 Analytical algorithms

From a clinical standpoint, analytical dose calculation models are the most practical method of estimating particle radiation transport in a particular medium. The pencil beam (PB) model is the most common approach to approximate the geometric and physical characteristics of particle beam dose-deposition (Hong et al. 1996). Figure 1.5 depicts a generalized case of a water phantom placed a distance from the particle beam-line, with rays (black), points (black, presenting BP positions) and target delineation (red).

Here, we describe the dose calculation of a voxel in a 3-dimensional (3D) geometry as

$$d(x,y,z) = \sum_{i=1}^{num_PBs} N_i \times IDD(z,E_0) \times G(x,y) \tag{1.14}$$

where for i number of indiviual PBs, each with a unique particle fluence (N_i), the central term IDD is the integral depth-dose curve as a function of depth in water (z_{eff}) of a particular initial beam energy E_0, and the auxiliary term G describes

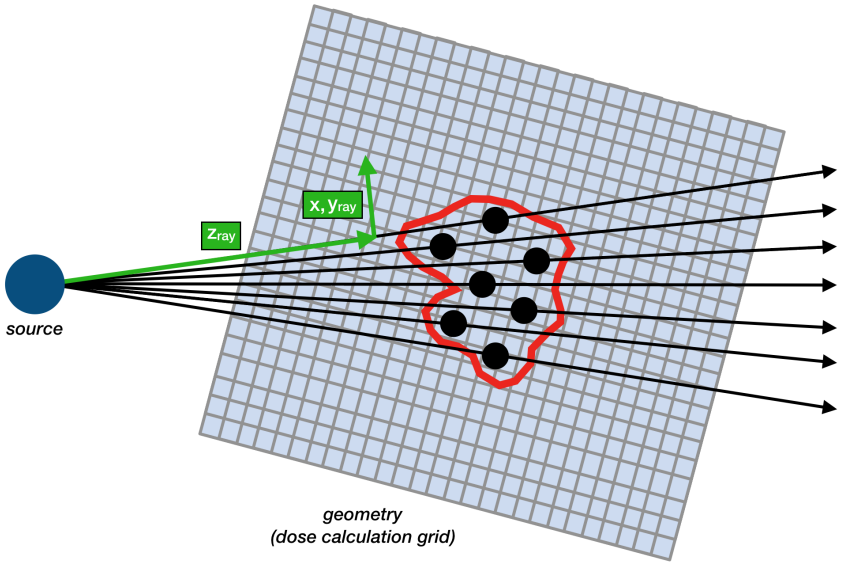

Figure 1.5 – Generalized dose calculation scenario with a beam-line and particular (homogeneous) volume. The black rays and points represent an individual ray-trace and corresponding BP position, respectively, with the target delineated in red.

the lateral evolution of the pencil beam, commonly modeled by a superposition of Gaussian functions. For each ray trace as depicted in Figure 1.5, $G(x, y)$ is computed for each voxel within the dose grid (neglecting dose cut-off/thresholds, e.g. 3 $\times\sigma$ for the highest order term). Subsequently, for a single PB, equation 14 can be expanded as

$$d(x,y,z) = N \times IDD(z, E_0) \times [(1-w) \cdot \mathrm{G}_1\left(r, \sigma_1\left(z_{\mathrm{eq}}, E\right)\right) + w \cdot \mathrm{G}_2\left(r, \sigma_2\left(z_{\mathrm{eq}}, E\right)\right)] \tag{1.15}$$

where G_1 and G_2 represent functions to describe a double Gaussian model, dependent on r $= \sqrt{x^2+y^2}$ and σ_i where i=1 and i=2, respectively, and the Gaussian weight (1-w) and (w) are the normalization factors for G_1 and G_2, respectively. Numerous works develop and implement models for lateral dose evolution of particular beams, such as double Gaussian (DG) (Parodi et al. 2013, Shen et al. 2016), triple Gaussian (TG) (Inaniwa et al. 2009, Inaniwa et al. 2014) and non-Gaussian approaches (Embriaco 2015, Bellinzona et al. 2016, Embriaco et al. 2017). Considering the generalized equation for a normal (Gaussian) distribution $G = \frac{1}{\sigma\sqrt{2\pi}} e^{-\frac{1}{2}((x-\mu)/\sigma)^2}$ and substituting into equation 15 yields the following:

$$d(x,y,z) = N \times IDD(z, E_0) \times \left[\frac{1-w}{2\pi\sigma_1^2} \cdot \int \mathrm{d}y \mathrm{e}^{\left(-\frac{x^2+\gamma^2}{2\sigma_1^2}\right)} + \frac{w}{2\pi\sigma_2^2} \cdot \int \mathrm{d}y \mathrm{e}^{\left(-\frac{x^2+\gamma^2}{2\sigma_2^2}\right)}\right] \tag{1.16}$$

Both the beam-spread in air from the nozzle (treatment head) to the surface entry and dose evolution within the medium can be modeled by Gaussian distributions. The initial beam spot-size is commonly characterized as a single Gaussian (SG) at the isocenter with a certain energy-dependent full width at half maximum (FWHM), where FWHM $= 2\sqrt{2\ln 2}\sigma$). Therefore, the contribution of beam spread by the various component can be expressed as the quadratic sum of the individual σ components

$$\sigma_{total} = \sigma_0^2 + \sigma_{air}^2 + \sigma_{medium}^2 \tag{1.17}$$

where σ_0 (initial spot size), σ_{air} (beam spread in air) and σ_{medium} (lateral dose evolution) can each be described as multi-Gaussian models. Recent works access the gains of implementing a triple Gaussian (TG) beam model into research-based or clinical dose engines (Inaniwa et al. 2014, Inaniwa et al. 2015, Embriaco et al. 2017). Figure 1.6 demonstrates importance of implementing higher order Gaussian fitting particle beams and the differing depth dose properties for the four ions available at HIT.

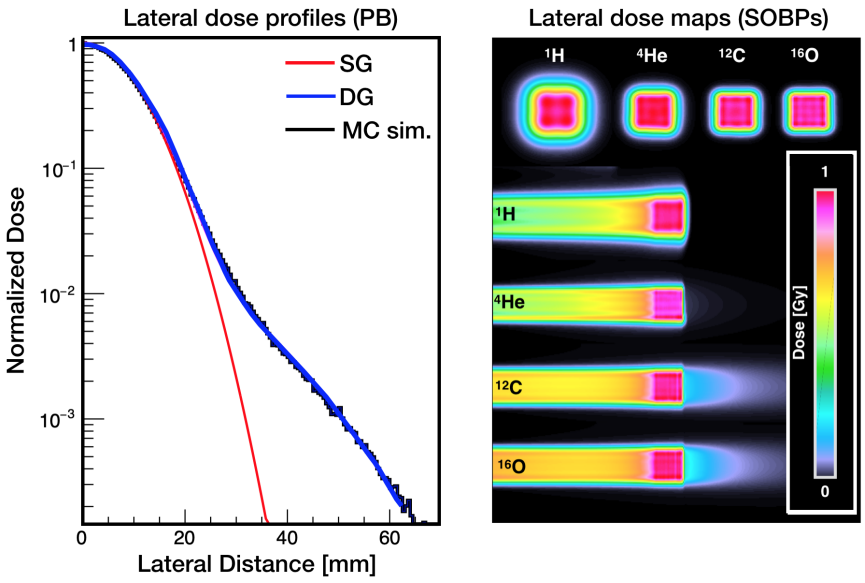

Figure 1.6 – Lateral dose evolution for a single pencil beam within the Bragg peak (mid-range energy proton beam). Monte Carlo against single Gaussian (SG) and double Gaussian (DG) fits (left). Depth dose and lateral dose maps for SOBPs (3x3x3 cm^3) for four ions (right).

In summary, a ray-trace is performed for each ray, determining distance from the source, and the water equivalent path length (WEPL) of each intercepted voxel. Subsequently, corresponding IDD and G parameters are computed for each contributing pencil beam. As opposed to Monte Carlo simulations, which can perform dose-to-medium (D_m) calculation, by incorporating known material compositions

for each unique material, analytical algorithms rely on beam-data collected during commissioning, usually characterized in water. Therefore, dose-to-water (D_w) is the standard clinical endpoint.

Particle interactions in homogeneous settings (infinite planar slab geometry) are well understood; however, limitations in analytical algorithms arise in scenarios with complex geometries and heterogeneities (spatial variation in anatomic density e.g. bone/tissue/air interfaces such as the skull-base or thorax region), which essentially accounts for every dose computation performed in the clinic outside the routine QA tests performed in homogeneous water phantoms and/or PMMA blocks. Therefore, it is critical for analytical codes to consider the effects of anatomic heterogeneities on the dose distribution.

Two main classes of heterogeneity handling have been proposed in previous reports: (i) ray casting and (ii) pencil beam splitting. Ray casting operates by correcting density heterogeneities with simple scaling of the water-equivalent depth (WED) of each dose grid calculation point along the field direction which "deforms" the pencil beam shape laterally. Pencil beam splitting offers an adaptable approach (variable/adaptive splitting multiplicity) and have the potential for high accuracy, but can be computationally intensive (Kanematsu et al. 2009, Russo et al. 2016). The mathematical formalisms applied in the presented thesis are detailed the *Appendix*. Each method has own its benefits and trade-offs. For example, ray casting methods are computationally fast and perform sufficiently well in handling superficial heterogeneities but may overestimate the effect of PB deformation (detailed in *Publication C*). PB splitting is adaptable and can yield a high degree of accuracy but may have issues producing effect of inhomegeneities close to the targets.

Recent efforts in particle therapy dose engines have focused on speed by pushing serial-based operations on the central processing unit (CPU) to parallelized computation on the graphic processing unit (GPU) (Jia et al. 2014). In terms of hardware, the advantages of a GPU over a CPU, is the large number of processing units. Despite GPU clock speed being relatively low compared to the CPU, the combined processing power can outperform CPU for most executions (i.e. when all GPU executions, which occur in parallel threads known as warps, process in the same execution path). For example, if-else functions may cause a warp diverge and put other threads in an idled state. This feature makes vector and matrix operations (e.g. analytical dose calculation algorithms) the ideal operation for GPU. In contrast, maintaining high speeds for GPU-based Monte Carlo codes is challenging due to the stochastic nature of modeling particle interactions, which would cause frequent divergent independent threads. Pseudo-code of CPU- versus GPU-based dose computation is shown below:

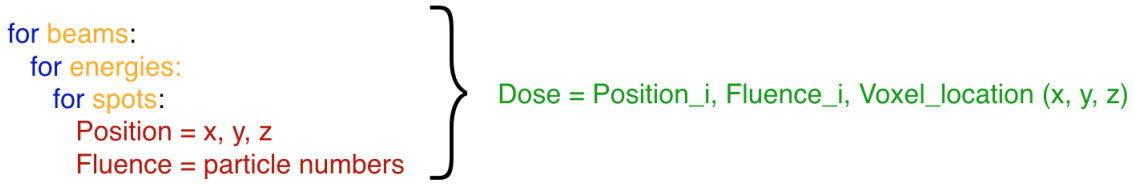

;

where a iterative loop of $x \times y \times z$ CPU-based processes can be replaced with a single execution on the GPU. From here, it becomes apparent that the iterative execution using an analytical PB dose calculation, with many kernels can be independently handled, are ideal for the GPU.

Physical dose is not the only parameter of interest for computation in particle therapy. Scoring additional metrics such as $\mathrm{LET_d}$ using analytical algorithms can occur on the fly:

$$LET_d = \frac{\sum_{i=1}^{N} D_i \times LET_i}{\sum_{i=1}^{N} D_i} \tag{1.18}$$

Similarly, computation of RBE-weighted dose requires dose-averaged scoring for parameters with:

$$\begin{aligned} \alpha_{\mathrm{mix}} &= \frac{\sum_i d_i \cdot \alpha_i \cdot w_i}{\sum_i d_i \cdot w_i} \\ \sqrt{\beta_{\mathrm{mix}}} &= \frac{\sum_i d_i \cdot \sqrt{\beta_i} \cdot w_i}{\sum_i d_i \cdot w_i} \end{aligned} \tag{1.19}$$

$$z^*_{1D\,\mathrm{mix}}(x) = \frac{\sum_i d_i(x) \cdot z^*_{1Di}(x) \cdot w_i}{\sum_i d_i(x) \cdot w_i} \tag{1.20}$$

such as α and β correspond to the linear and quadatric terms of the LQ-model, while $z^*_{1D\,\mathrm{mix}}(x)$ represents the saturation-corrected dose-mean specific energy.

1.6 Aim of the thesis: development, validation and application of FRoG

Currently in the clinic, there is an absent pipeline for efficient testing and implementation of innovative models, advanced computation and new-age treatments in particle therapy. As previously stated, the clinical standard worldwide for effective dose prescription and treatment planning in proton therapy assumes a constant RBE of 1.1, a conservation estimate despite evidence of variable RBE and high-LET effect along the BP (Paganetti et al. 2002, Chaudhary et al. 2014, Peeler et al.

2016). For carbon ions, facilities like HIT implemented LEM-I, which is still in clinical use today (Combs et al. 2010) despite more update-to-date versions presenting substantially different predictions (Gillmann et al. 2019). Moreover, both leading modalities in particle therapy have yet to integrate LET-related effects into clinical decision-making. The clinical TPS is often a "black box" program which does not afford flexibility for in-house development. Recent works developed or expanded secondary systems in-house (e.g. TRiP, Astroid, matRad and FoCa) and benchmarked against their model center's clinical treatment planning system (TPS) for educational purposes or clinical support (Wieser et al. 2017, Sánchez-Parcerisa et al. 2014, Krämer et al. 2016, Kooy et al. 2010). However, the accuracy of such pencil-beam (PB) algorithms may be less than satisfactory in challenging patient cases with considerable heterogeneity. Moreover, most platforms, like the clinical TPS, have limited flexibility and speed (CPU-based) when advanced metrics are desired (e.g. $\mathrm{LET_d}$ and $\mathrm{D_{RBE}}$) for studying large patient cohorts. Monte Carlo simulations can however support clinical and research investigations in radiotherapy, but most codes cannot meet the needs of the clinic and require extensive physics and programming expertise. Therefore, recent efforts have focused on increasing speed of accurate yet time intensive codes for proton therapy by pushing to the GPU (Jia et al. 2012a, Jia et al. 2014).

In this work, we present the **Fast Robust dose calculation on GPU (FRoG)** platform, initially developed in-house at HIT in 2018 as a GPU-based auxiliary analytical dose engine to support research and clinical activity at HIT for the four ions available: protons (^{1}H), helium (^{4}He) ions, carbon (^{12}C) ions and oxygen (^{16}O) ions (Mein et al. 2018, Choi et al. 2018). As depicted in Figure 1.7, FRoG is a multi-purpose sandbox environment written in `python` and `C++` to perform rapid and accurate computations using a PB model (Hong et al. 1996) with triple Gaussian lateral evolution parameterization (Inaniwa et al. 2009, Inaniwa et al. 2014) and GPU-optimized Siddon raytracing (Siddon 1985) for physical dose, $\mathrm{LET_d}$, RBE and effective dose. The FRoG project began as a collaboration project between HIT and the National Centre for Oncological Hadrontherapy (CNAO, Pavia, Italy) but has expanded to additional centers in Europe. FRoG aims to support both large research institutions and smaller clinics which lack the resources and man-power to establish a substantial research support team locally within the clinic.

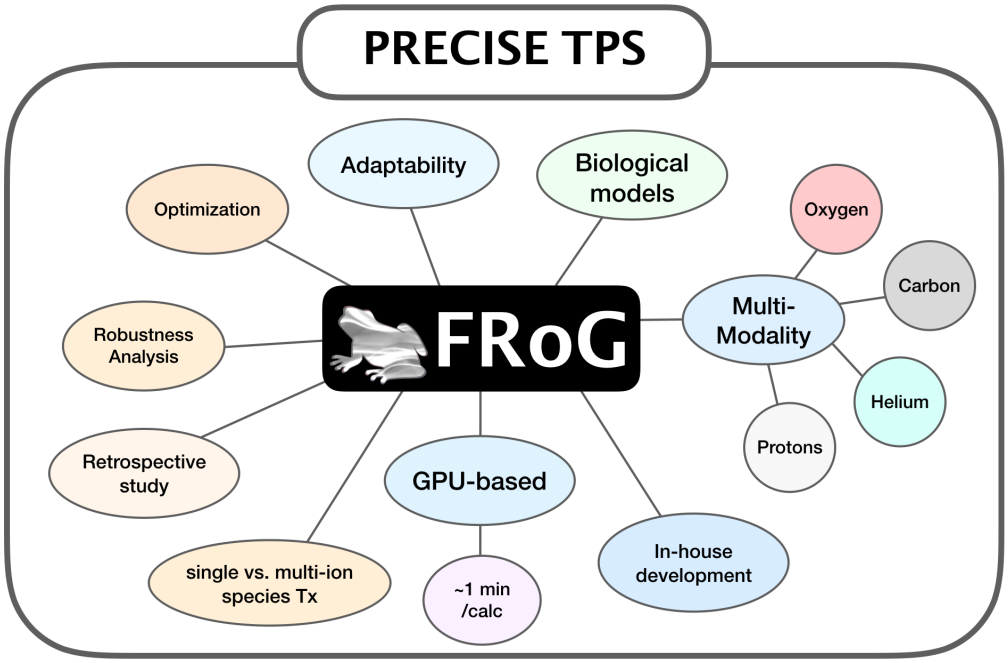

Figure 1.7 – FRoG diagram detailing base features and functionality.

The publications collected for the cumulative thesis detail the development, validation and application of FRoG for various research and clinical scenarios in particle therapy. The main aims of the thesis, addressed in the four published works, are as follows:

i. development of a fast GPU-based analytical dose engine for various modalities in particle therapy (FRoG).

ii. validation of various particle therapy dose engines (both Monte Carlo and analytical) in both homogeneous (simple) and heterogeneous (clinical-like) settings.

iii. Applications of FRoG to support clinical and research activity at two distinct hadrontherapy facilities (HIT and CNAO).

Lastly, future works and challenges regarding the development and application of fast robust dose engines in ion therapy are explored in the *Discussion* section.

2 Publications

This thesis is presented in 'cumulative' format in accordance with the regulations of the Department of Physics and Astronomy of Heidelberg University. It comprises four articles published in internationally recognized peer-reviewed journals. The individual manuscripts are referred to within this thesis with alphabetical ordering (A, B, C, and D). The dissertation is part of the FRoG collaboration formed between HIT and CNAO in 2017. All work was performed in close collaboration with Kyungdon Choi (CNAO, Pavia, Italy), Benedikt Kopp (DKFZ, Heidelberg, Germany) and PD. Dr. Andrea Mairani (HIT, Heidelberg, Germany). The main focus of the thesis is Heidelberg-based development, methodologies, experimental validation, and applications. The secondary focus of the thesis involved external collaborations and applications (mainly in Pavia, Italy and Caen, France). Specific author contributions to each article are stated in the respective following sections. A timeline is displayed in Figure 2.1 labeled with corresponding publications (A-D).

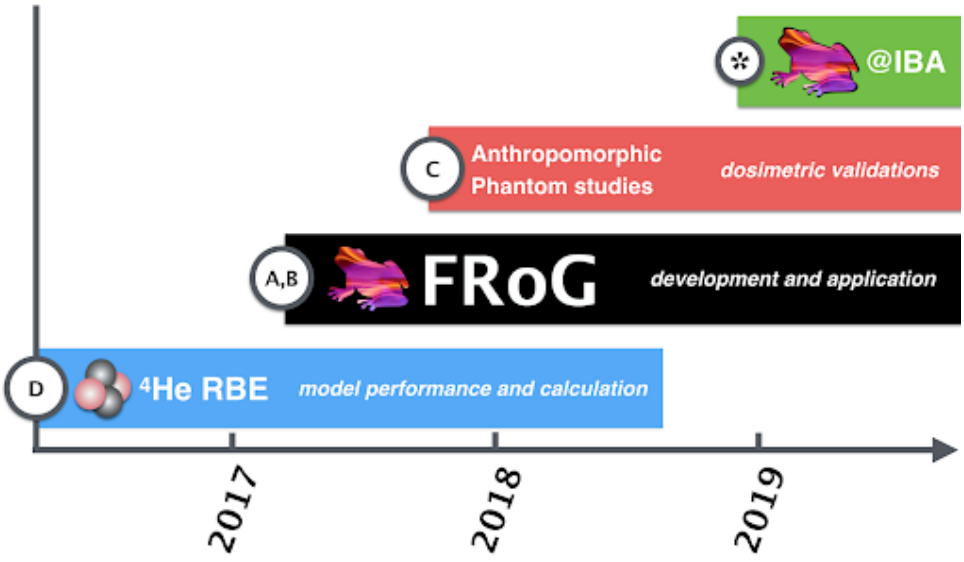

Figure 2.1 – Timeline of projects and related publications. Note: (*) indicates ongoing projects which are presented in the *Discussion* section.

A Fast robust dose calculation on GPU for high-precision ^{1}H, ^{4}He, ^{12}C and ^{16}O ion therapy: the FRoG platform

Authors: Stewart Mein, Kyungdon Choi, Benedikt Kopp, Thomas Tessonnier,, Julia Bauer, Alfredo Ferrari, Thomas Haberer, Jürgen Debus, Amir Abdollahi, Andrea Mairani

Publication status (10/2018): Published **Journal reference:** Scientific Reports 8, Article number: 14829

DOI: 10.1038/s41598-018-33194-4

Authors' contributions: SM is the first author of this publication. SM performed all of the presented computations (both analytically and via simulation), wrote the main manuscript, constructed all figures and co-developed the FRoG program (which involved programming in PYTHON and C++, both CPU- and GPU-based). BK and KC are co-developers with A.M. as lead designer of project FRoG. TT, JB and AF contributed to data acquisition through support with FLUKA MC simulation. TH, JD and AA provided clinical direction during project development and manuscript writing.

B FRoG—A New Calculation Engine for Clinical Investigations with Proton and Carbon Ion Beams at CNAO

Authors: Kyungdon Choi, Stewart Biedeman Mein, Benedikt Kopp, Giuseppe Magro, Silvia Molinelli, Mario Ciocca, Andrea Mairani
Publication status (10/2018): Published **Journal reference:** Cancers 2018, 10(11), 395
DOI: 10.3390/cancers10110395

Authors' contributions: SBM co-wrote the manuscript alongside first author (CK) the senior author (AM). SBM co-developed the FRoG platform for LET and RBE-weighted dose calculation alongside KC, BK and AM (involving programming in PYTHON and C++). GM contributed to data acquisition through support with FLUKA MC simulation. SM performed the Syngo plans. SM and MC provided clinical direction during project development and manuscript writing.

C Dosimetric validation of Monte Carlo and analytical dose engines with raster-scanning ^{1}H, ^{4}He, ^{12}C and ^{16}O ion-beams using an anthropomorphic phantom

Authors: Stewart Mein, Benedikt Kopp, Thomas Tessonnier, Benjamin Ackermann, Swantje Ecker, Julia Bauer, Kyungdon Choi, Giulia Aricò, Alfredo Ferrari, Thomas Haberer, Jürgen Debus, Amir Abdollahi, Andrea Mairani
Publication status (07/2019): Published **Journal reference:** Physica Medica: European Journal of Medical Physics, Volume 64, 123 - 131
DOI: 10.1016/j.ejmp.2019.07.001

Authors' contributions: SM performed all of the presented analysis, wrote the main manuscript, constructed all figures and co-developed the FRoG program for the four ions presented in this work (1H, 4He, 12C, and 16O). SM led and carried out all experimental aspects of the study (dosimetric measurements) with the assistance of co-authors BK and TT. BA and SE provided medical physics support during measurement acquisition and clinical TPS computations. GA and AF contributed to data acquisition through support with FLUKA MC simulation. TH, JD and AA provided clinical direction during project development and manuscript writing.

D Biophysical modeling and experimental validation of relative biological effectiveness (RBE) for ^{4}He ion beam therapy

Authors: Stewart Mein, Ivana Dokic, Carmen Klein, Thomas Tessonnier, Till Tobias Böhlen, Guiseppe Magro, Julia Bauer, Alfredo Ferrari, Katia Parodi, Thomas Haberer, Jürgen Debus, Amir Abdollahi, Andrea Mairani
Publication status (10/2018): Published **Journal reference:** Radiation Oncology 14, Article number: 123
DOI: 10.1186/s13014-019-1295-z

Authors' contributions: SM performed all of the presented analysis, co-wrote the manuscript alongside the senior author (AM) and constructed all figures. I was responsible for performing all steps involving Monte Carlo simulation, in vitro clonogenic cell survival assay (under the supervision of co-authors ID and CK) and development of the FRoG platform for helium ion beam dose computation (involving programming in PYTHON and C++). TT, TTB, AF and KP contributed to data acquisition through support with FLUKA MC simulation. GM contributed to data acquisition through support with RBE modeling. TH, JD and AA provided clinical direction during project development and manuscript writing.

3 Discussion

In this chapter, the key concepts, findings and achievements for dose calculation in particle therapy are discussed and are contextualized within the current state of the relevant literature. From the four published works which comprise the cumulative thesis, the major aims achieved are as follows. A GPU-accelerated analytical dose engine for p, ^{4}He, ^{12}C and ^{16}O ion therapy (FRoG) was developed. Its dose calculation performance was evaluated experimentally for both homogeneous and heterogeneous settings as well as in relation to other existing Monte Carlo and analytical systems at two distinct hadrontherapy facilities (HIT and CNAO). Finally, the biophysical phenomena of a novel treatment modality using ^{4}He ion beams are investigated to integrate relevant models (both physical and biological) and to establish a framework for research and clinical support using FRoG. Additionally, future and ongoing efforts in the development and application of fast robust dose engines in ion therapy are explored in this chapter.

FRoG does not only provide an auxiliary platform for physical dose computation, but also clinical metrics which are currently unavailable in the standard commercial TPS such as $\mathrm{LET_d}$ and RBE-weighted dose with innovative models (biophysical/mechanistic and phenomenological). As proof of principle, Figure 3.1 depicts biological dose computation for three particle therapy plans optimized with protons, helium ions and carbon ion beams. The proton plan was initially optimized and calculated assuming RBE of 1.1 as performed in the clinic, and subsequently, a forward calculation was performed using a phenomenological (data-drive) variable RBE model Mairani et al. 2017b. The second plan (rightward) considers the differing biological perspective between Europe and Japan for model variable RBE with carbon ions, by performing forward calculations of a chondrosarcoma patient plan (previously treated at HIT, optimized with LEM-I) with MKM. These three case studies each provide a unique perspective on the value of systems like FRoG which readily allow testing of different models and metrics. That is, $\mathrm{LET_d}$ and variable RBE schemes are currently absent in the clinical decision making process for proton therapy and the AAPM TG-256 report suggests restructuring of the current simplistic workflows for proton therapy. For the heavier ions, RBE model selection should not be taken lightly since the clinical model will influence routine procedure

and clinical outcome. The following sections will discuss FRoG's performance as an auxiliary dose engine in relation to other systems (both clinical and research based) as well as gold standard measurements. It will also evaluate clinical potential for systems to introduce advanced metrics and models (i.e. LET and variable RBE for proton therapy) and explore the ongoing and potential studies such as clinical outcome investigations and novel treatment delivery and verification technique development using FRoG. Finally, applications beyond Heidelberg and future visions for FRoG are considered.

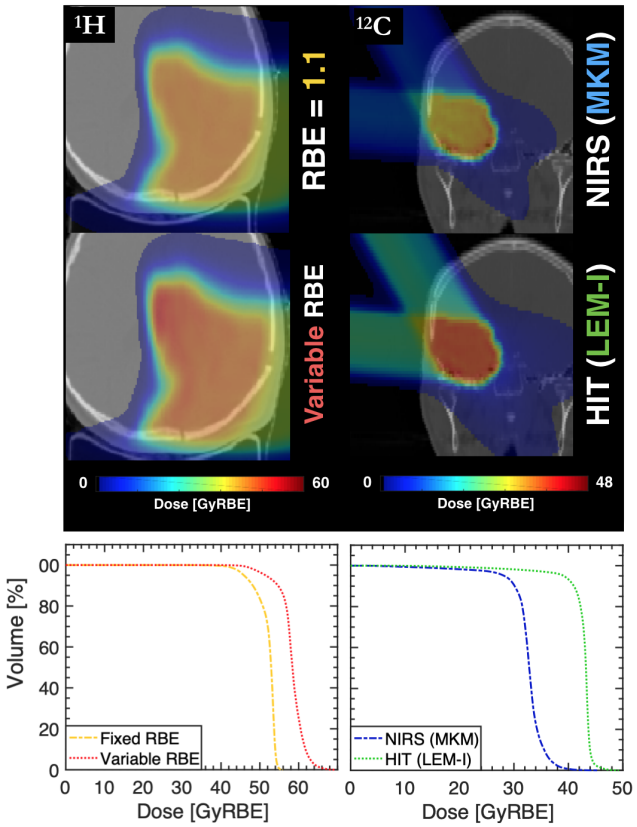

Figure 3.1 – Comparison of effective dose prediction schemes for clinical particle beams. Dose maps for a skull base chordoma patient (left) treated with protons ("patient A" from *Publication A*) and carbon ions ("patient D" from *Publication A*) at HIT. For the proton case, the clinically assumed constant RBE = 1.1 and a variable RBE model (Mairani et al. 2017a) are applied. For carbon ions, the NIRS- and HIT-based approaches (MKM and LEM-I, respectively) are applied.

3.1 Performance as an auxiliary dose engine

Publication A presents the development and initial validation of FRoG against FLUKA Monte Carlo simulations (the same Monte Carlo code used for FRoG base

data generation i.e. energy dependent integral depth dose profiles and lateral dose evolution) in both homogeneous and heterogeneous conditions (water phantom and patient cases) for the four ions available at HIT. Validation of SOBP plans in water demonstrated excellent agreement with FLUKA Monte Carlo within ~1% for protons and ~2% for the heavier ions. The initial validation demonstrated the accuracy improvements with using higher-order lateral dose evolution parameterization (i.e. DG vs. TG), particularly for the helium, carbon and oxygen ions. As for FRoG's performance with patient calculations, its accuracy stems from dual pencil beam (DPB) model and sub-pencil beam superposition as described in the *Appendix* section of the thesis. First detailed in *Publication A*, the DPM model is a unique approach to the PB algorithm to separately handle primary particles interacting in the beam applications and monitoring system (BAMS), which for the lighter particle beams (protons and helium ions) induces large angle scattering and, in turn, a substantial low-dose envelope. Consequently, the DPB model yields improved accuracy against to Monte Carlo predictions when compared to conventional PB algorithms in heterogeneous structures but at the cost of increased run-times. The DPB model is, however, specific to the HIT beam-line, and therefore, the times provided in table 1 of *Publication A* are higher than one would anticipate from a GPU-based analytical code, with an average ~170 seconds per patient for the four ions. It should be noted that the computation times account for physical dose, as well as $\mathrm{LET_d}$ and several RBE-weighted doses. Therefore, in the context of FRoG's performance for other centers, the average forward calculation of a patient case would take approximately one minute, maintaining the same degree of PB subdivision. Moreover, as stated in *Publication A*, dose kernel run-times per PB were in line with RayStation.

The initial development and validation of FRoG at HIT was accompanied by *Publication B*, which presents FRoG predictions at CNAO for physical dose, $\mathrm{LET_d}$ and effective dose as well as a validation of physical dose in various homogeneous settings (SOBPs with varying field size and depth) for the clinical beams (protons and carbon ions). In short, a dosimetric study of SOBP plans irradiated in a water tank presented the following results: for proton beams, FRoG and SyngoPT® were in agreement with ion chamber measurements within 0.7% an 1.0%, respectively. For cases with the range shifter in-place, agreement was within 1.1% for FRoG and 1.4% for SyngoPT®. Additionally, a dosimetric study was performed for twenty-five patient-specific QA fields irradiated in the water tank. Differences between calculated and measured dose over the all fields were $1.96(\pm 0.79)\%$ for FRoG and $2.71(\pm 1.25)\%$ for SyngoPT®. Similar results were recorded for carbon ions. Finally, *Publication B* introduced $\mathrm{LET_d}$ and RBE-weighted dose computations (using both Japanese- and European-based approaches) for protons and carbon ions, respectively, which demonstrated excellent agreement with Monte Carlo simulation.

Following the developmental and validation works, *Publication C* details a unique dosimetric study at HIT with a challenging half-head anthropomorphic phantom set-up for p, $^{4}\mathrm{He}$, $^{12}\mathrm{C}$ and $^{16}\mathrm{O}$ ion beams. FRoG was validated with both 1D and

2D ionization chamber measurement devices, with its performance tested against full Monte Carlo simulation and a commercial TPS (SyngoPT®) for particle therapy. The dosimetric measurements acquired during the study (especially with the OCTAVIUS® system) were particularly valuable since they represent the first measurements taken in anthropomorphic settings for ^{4}He, ^{12}C and ^{16}O ion beam therapy. Acquiring useful measurements in the distal-end/fall-off are challenging considering range uncertainty in particle therapy. Additional tests are recommended in the near future to verify range prediction and dose within the fall-off region for anthropomorphic phantom set-ups. Considering the upcoming clinical trials with helium ion at HIT, FRoG shows promise as a viable analytical engine for helium ions, validated against Monte Carlo and *in vitro* measurements for helium ion beam therapy (Mein et al.), making way for next-generation modeling and dose computation. These topics are discussed further in the sections that follow.

Performance of in-house systems (MCTP and FRoG) as well as the current clinical TPS at HIT (SyngoPT® by Siemens, Erlangen, Germany) in heterogeneous conditions is of particular importance since its a test which is more representative to the clinical condition (patient anatomy) than homogeneous settings with a water phantom and rectangular parallel-piped SOBPs. Simple tests are of course vital for initial benchmarks, but by performing rigorous tests in this manner, systematic errors or trends may become more apparent which are not routinely visible during quality assurance (QA) procedures. For example, the SyngoPT® forward computation of the proton SOBP behind the anthropomorphic has a distinct visual appearance and visibly differs from the other computation methods (full Monte Carlo and analytical pencil beam splitting codes). We conclude in this work that the MCTP and FRoG performed well in challenging conditions, as demonstrated by superior agreement with measurements (generally within ~2% to ~3%) for the four ions, while SyngoPT® presented clinically relevant discrepancies for the proton field. As elaborated in *Publication A*, FRoG compensates for the particular beam-line by (i) TG parameterization of the lateral dose evolution and (ii) separately modeling primary particles which interact in the BAMS from the pristine primary beam with the DPB model.

Another intriguing experiment involved the in-house double-wedge phantom, which tests dose calculation performance in anatomically complex scenario (Fig. 3.2). In this test, plan optimization was performed using SyngoPT® and therefore the dose map and profiles are homogeneous within the target of the SyngoPT® calculation. Similar to the half-head anthropomorphic phantom investigations in *Publication C*, MCTP and FRoG produced comparable distribution but with hot-spots generated at the distal-end and variations observed up to ~15% in the target when compared against SyngoPT®.

The Siemens system was first developed in mid-2000's and based on a ray-casting method called WEPL-to-POI. Depending on the approach to implementation and the modeled beam-line, dose distribution prediction using WEPL-to-POI in complex

geometries and for oblique beam angles, may present clinically relevant differences compared to gold standard Monte Carlo simulations and measurements. End-of-range measurements are especially challenging due to various factors like HU-WEPL conversions using convectional CT methods used in the clinic. Moreover, Siemens is no longer supporting development for SyngoPT®. For these reasons, installation and validation of more update-to-date systems like RayStation® (RaySearch, Stockholm, Sweden) are underway at HIT for treatment planning with protons and carbon ions. Ongoing works will expand on the measurements from *Publication B* and *Publication C* by including a more modern clinical TPS.

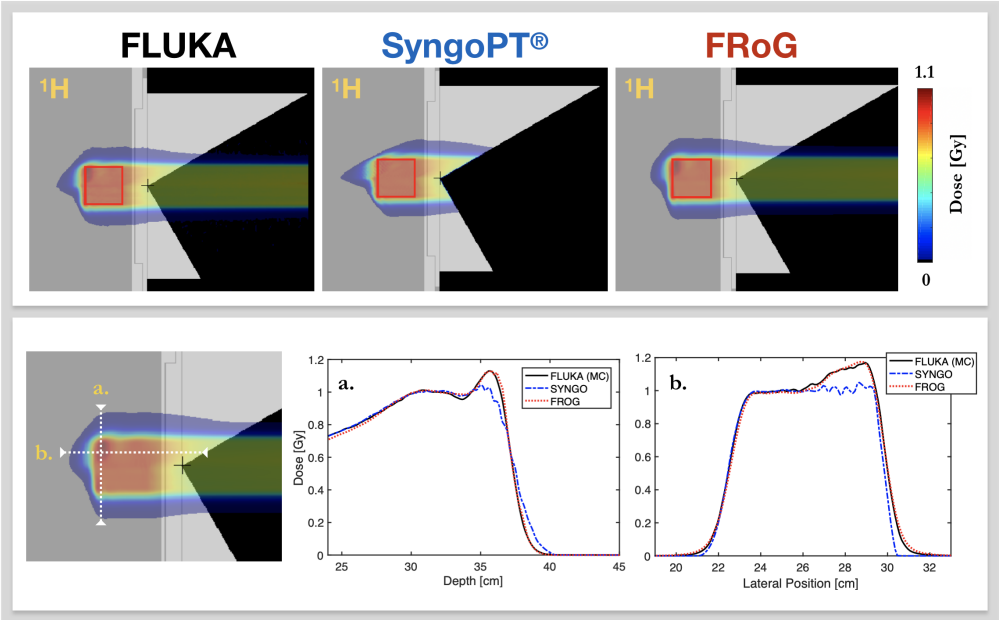

Figure 3.2 – Dose calculation performance testing (FLUKA vs. SyngoPT® vs. FRoG) with the double-wedge phantom. Dose maps (top) and line profiles (bottom), depth-wise and lateral, are provided. With the plan optimized using SyngoPT®, SyngoPT® predicts a relatively homogeneous dose distribution within the target. However, this results is no poor agreement demonstrate FLUKA and FRoG, which predict hot-spots at the distal end, up to approximately 15%. WEPL-to-POI may have performance issues for oblique beam angles and geometric planes.

In the field of radiotherapy, there is a rising interest in secondary dose engines for clinical QA purposes. IBA and research scientists from SciMoCa™ teamed up in 2018 to bring an auxiliary Monte Carlo verification tool to photon and electron therapies (Ion Beam Applications S.A. 2018b). Related works in the literature develop and evaluate the role of machine learning to perform so-called "virtual QA" and its potential impact on clinical dose computation and workflows in the photon world (Valdes et al. 2016, Valdes et al. 2017). However, extensions to particle therapy dose engines have yet to be made commercially available. Such systems could greatly streamline the tedious and redundant QA procedures. The role of secondary dose

engines like SciMoCa^{TM} and FRoG are expected to become more commonplace in clinical environments.

Other GPU-based analytical engines (Da Silva et al. 2015, Fujimoto et al. 2011) have been developed for proton therapy, most notably a recent ray-casting algorithm capable of dose calculation and optimisation within 10 seconds (Matter et al. 2019). As for fast Monte Carlo, several GPU-based codes have been published to support clinical and research activity at their respective facility (Kohno et al. 2011, Yepes et al. 2010, Jia et al. 2012a, Wan Chan Tseung et al. 2016, Schiavi et al. 2017, Li et al. 2017, Maneval et al. 2019). Apart from `goCMC` (Qin et al. 2017, Qin et al. 2018) which performs GPU-based Monte Carlo prediction for carbon ions, existing platforms are specific to proton beams, preserving the accuracy of the Monte Carlo while substantially reducing computation times. Several works propose and investigate the value of patient-specific QA using treatment delivery log files recorded after each fraction (Zhu et al. 2015, Scandurra et al. 2016, Chung 2017, Johnson et al. 2019). There is currently no streamlined protocol in particle therapy clinics to access and perform quick computations using these patient-specific log files; however, secondary systems like FRoG have demonstrated their capacity to handle log files and, through rapid GPU-accelerated dose calculation, to access the impact of daily fluctuations in treatment delivery parameters and uncertainties, e.g. fluence, spot position and foci (Mein et al. 2018).

Several publications speculate the clinical impact of auxiliary systems, the future role of variable RBE dose calculation in proton therapy and follow up with an extension of the code to partnering centers, such as `FRED` at the Krakow proton beam therapy centre (Garbacz et al. 2019) and `FDC` at the Shanghai Proton and Heavy Ion Center (Wang et al. 2018). Similarly, FRoG was initially developed through the HIT/CNAO collaboration and has been recently installed at Danish Centre for Particle Therapy (DCPT) at Aarhus University Hospital (Skejby, Denmark) and the Normandy Proton Therapy Center at François Baclesse Centre (Caen, France) to support clinical and research activity (Fig. 3.3). Adaptation and intial validations at the Normandy facility will be discussed in following sections.

3.2 Environment for advanced metrics and models: LET and RBE

To this day, there is no commercial TPS which provides LET_d prediction in the clinic. In the case of protons, the standard clinical TPS provides a single biological perspective (constant RBE = 1.1). The past decade has seen a myriad of works publish *in vitro* (Paganetti et al. 2002, Chaudhary et al. 2014, Paganetti 2012), *in vivo* (Saager et al. 2018, Sørensen et al. 2011) or in man, providing evidence of observed LET_d effects (Peeler et al. 2016, Carabe et al. 2013). Other works evaluated the

Figure 3.3 – FRoG Partnership map — besides the Heidelberg Ion-beam Therapy Center (HIT), FRoG is supporting clinical and research activities the National Centre for Oncological Hadrontherapy (CNAO, Pavia, Italy), the Danish Center for Particle Therapy (DCPT, Aarhus, Denmark) and the Normandy Proton Therapy Center (Caen, France). FRoG is functional for both synchrotron- and cyclotron-based facilities including Siemens, Varian ProBeam® and IBA ProteusOne® beam-lines.

impact of a variable RBE in proton therapy clinical trials using different fractionation schemes (Dasu and Toma-Dasu 2013, Marshall et al. 2016), concluding that the current clinical assumption most likely overestimates the therapeutic ratio in proton therapy for liver cancer (Chen et al. 2018). These works should prompt swift action by clinical environments to incorporate LET optimization into treatment planning, or at the very least treatment selection based on favorable LET estimations (i.e. reduced high LET in OARs or sensitive normal tissues) (Unkelbach et al. 2016, Unkelbach and Paganetti 2018). LET-based optimization techniques have been shown to substantially reduce dose-response uncertainty (McMahon et al. 2018).

Notably, the effect of improper RBE assignment is not simply a tumor control issue but manifests in the risk for normal tissue toxicity (Lühr et al. 2018, Jones et al. 2018). For instance, clinicians implement safety margins beyond the clinical target volume (CTV) which comprises the disease bed; however, the effective range and penumbra, especially at the distal end, may be expanded due to the increased effective dose in high-LET regions which potentially jeopardizes efforts to reduce toxicity (Carabe et al. 2012, Giovannini et al. 2016). Recent reviews outline clinical implementation of variable RBE prediction as a move towards more personalised treatment, especially considering inter-tumoral genomic heterogeneity, including DNA damage response, is increasingly appreciated as a major contributor to variation

treatment response (Willers et al. 2018). Despite these extensive works, considerable variability in both RBE measurement (*in vitro* and *in vivo*) and prediction remains. Furthermore, many studies vaguely report physics and dosimetry parameters used during radio-biological studies, which ultimately stunts reproducibility of much needed data for proton RBE (Draeger et al. 2019).

In response to these immediate clinical issues, several phenomenological-based RBE models for proton therapy have been published in the last decade, each with a unique approach and tuned to an existing *in vitro* dataset (Wilkens and Oelfke 2004, McNamara et al. 2015, Wedenberg et al. 2013, Mairani et al. 2017b, Carabe-Fernandez et al. 2007, Chen and Ahmad 2012, Unkelbach et al. 2016, Frese et al. 2011). These models are well summarized in a recent review (Rorvik et al. 2018) and analyzed with respect to the clinical dose, LET and reference radiation fractionation sensitivity range. With respect to *in vivo* dose-reponse, other works either measure (Saager et al. 2018) or model RBE for clinically relevant endpoints (Lühr et al. 2017).

From a practical standpoint, the first step requires driving such metrics to the clinical spotlight with fast, user-friendly dose engines such as FRoG. From here, $\mathrm{LET_d}$ and RBE models should be evaluated as a link to clinical outcome in patients. Novel works propose and implement a mixed RBE model (MultiRBE) approach in matRad, where uniform constant and variable RBE are applied in the target contours and normal tissues, respectively (Sánchez-Parcerisa et al. 2019). The Multi-RBE is one approach to incorporate variable RBE models in the clinic without severely altering the current method of planning tumor coverage. Other works present a Monte Carlo based framework to model radiation response for assessment of clinical RBE variability in proton therapy (Eulitz et al. 2019).

Similarly, FRoG provides an intuitive platform for computing these advanced metrics for four ions (p, ^{4}He, ^{12}C and ^{16}O). Choi et al. demonstrated that FRoG predictions for LETd values were in good agreement with Monte Carlo (within 0.3 keV $\mu\mathrm{m}^{-1}$ in both the target and OARs). For carbon ions, both MKM- and LEM-based DRBE calculations were implemented and validated against Monte Carlo to support dose conversion between facilities using different biological perspectives.

As previously stated, FRoG is used during clinical operation at the Danish Center for Particle Therapy (DCPT, Aarhus, Denmark), with other facility partnerships planned or pending (Fig. 3.3). Upcoming works will provide a detailed account of the adaptation, commissioning, and application of a fast (GPU-based) independent dose calculation system for Varian and IBA-based proton therapy centers. As for related GPU-based projects, future efforts will develop and investigate next-generation models with patient-specific clinically-accessible parameters such as measurable cell or tumor micro-environment characteristics (Oesten et al. 2019, Arnold et al. 2018, Chiblak et al. 2019).

FRoG is ideal for fast assessment of comparative treatment plans of different ion species, both prospectively and retrospectively with a large treatment diversity (e.g. particle species, beam angles, number of beams), using robustness analysis and large patient cohorts. To overcome uncertainties of actual in-vivo physical dose distribution and biological effects elicited by different radiation qualities, a flexible dose engine like FRoG can serve as a sand-box environment for testing innovative models prior to clinical integration. This is particularly vital for upcoming clinical trials (e.g. pancreatic) and introducing novel modalities to the clinic like raster-scanning helium ion beams.

3.3 Investigating RBE for helium ions

An imminent internal application of FRoG is to support research and clinical activity during the start-up of the raster-scanning helium ion beam therapy program at HIT by 2020. As discussed in *Publication D*, helium ions exhibit favorable physical and biophysical characteristics i.e. intermediate qualities between protons and carbon ion fields, such as a reduced lateral scattering/penumbra and enhanced biological effects compared to protons, with a reduced fragmentation tail compared to carbon ions (Tessonnier et al. 2017c). Revisiting *in vitro* dose-response for helium ion beams through the investigation of a cell line with a clinically relevant (α/β_x) was a main achievement of this work. Clonogenic cell survival assays were preformed following the in-house protocol (Dokic et al. 2016) to test three RBE models for helium ions, incorporated into a detailed FLUKA Monte Carlo simulation for the 96-well plate: DDM (Mairani et al. 2016a), LEM-IV (Grün et al. 2012) and MKM (Inaniwa et al. 2010, Mairani et al. 2017b). Finally, RBE model performance was tested in silico for patient cases and used to verify GPU-accelerated effective dose computation. FRoG landmarks the first GPU-based dose engine for helium ions.

Since the shut-down of many clinical trials using helium ions at LBL decades prior (apart from ocular melanoma which continued for several years after (Castro et al. 1997)), helium ion beams remain clinically unexploited. In short, the results of the clinical trials were as follows: helium ions were advantageous when irradiating smaller tumors, traditionally treated with photon/electron-based treatments, situated near radio-sensitive tissues (e.g. chondrosarcoma, melanoma, etc.). Conversely, large tumors did not respond well to helium ion radiation and due the lack of substantial evidence of improved local control and survival using helium-ion therapy, most trials were closed followed by pilot trials using heavier ions such as neon (^{20}Ne) ions, e.g. for pancreas carcinomas (Saunders et al. 2006, Linstadt et al. 1988). Due to the relatively simplistic treatments compared to modern-day planning and delivery methods (which assumed a constant RBE of 1.3 and used passive-scattering techniques), one could speculate that, given the knowledge and capabilities of the time-period, the clinical trials could not fully exploit the clinical

potential of helium ions, leading to a relatively poor outcome compared to heavier ions. One interpretation of these trial results relates to target volume dependency of clinical outcome, since, for particle treatments, a tumor will experience heterogeneous, spatially-variant LET across the treatment volume. Depending on tumor shape/volume and selected field configuration for delivery, regions of the tumor may experience substantially different $\mathrm{LET_d}$ and in turn, volume/RBE dependent effects. For example, covering large target volumes requires many overlapping energy slices and, compared to smaller targets, involves greater overlapping of entrance channel dose with relatively low LET parts ($<$ 10 keV) for helium ion beams.

Despite the lack-luster conclusions from the LBL clinical trials, a revival of interest in helium ion beam therapy is taking place, with several publications added to the literature and key-note talks presented at various international conferences in the recent years (Ströbele et al. 2012, Fuchs et al. 2012, Fuchs et al. 2015, Mairani et al. 2016a, Mairani et al. 2016b, Krämer et al. 2016, Knäusl et al. 2016, Tessonnier et al. 2017c, Tessonnier et al. 2018). It is therefore valuable to revisit the basic features of helium ion beams, not only in the context of the improved treatment delivery techniques e.g. active scanning, but also in relation to the complex biological effects and modeling variable RBE for treatment planning. An important question to ask is the following: with nearly two decades of light and heavy ion treatments, what have we learned from a constant RBE for protons and variable RBE for carbon ion beams to best implement a novel modality such as helium ion beam therapy?

Recent works (including a doctoral thesis) performed extensive dosimetric characterizations of helium ion beams (Tessonnier et al. 2017b, Tessonnier 2017). Several SOBPs in water (ranging in field size and depth) were simulated and measured in homogeneous settings (Tessonnier et al. 2017a). For improved modeling of helium ion beams, particularly for higher energies where integral depth dose deviations near the BP were detected on the order of ~6% (Tessonnier et al. 2017c), recently acquired cross-section measurements were incorporated into the FLUKA Monte Carlo simulation code (Horst et al. 2019) and validation is currently underway. *Publication C* took further steps to evaluate the current status of simulating helium ion beams with Monte Carlo methods and PB analytical algorithms in heterogeneous settings. Through dosimetric investigations, this work constitutes the first measurements for helium ion beams using anthropomorphic phantom set-ups. In such cases, we found that uncertainty in physical dose prediction for helium ion beam is on the order of ~3%.

Publication D, on the other hand, determined biophysical uncertainties of roughly 5% to 10% depending on the end-point, RBE model, investigated tissue type. The work presented in *Publication D* is a continuation of previous work by first outlining the short- and long-term goals for understanding RBE for helium ion beams, depicted in Figure 3.5. Currently, there exists two clinical approaches to modeling variable RBE for particle beam: LEM is applied at centers in Europe and China, while MKM is applied in Japanese-base facilities. A modified MKM was recently made

available to best reproduce *in vitro* cell survival data in clinically-relevant scenarios for proton and ^{4}He ion beams (Mairani et al. 2017b). A recently developed "data-driven" phenomenological model for helium ion beams provides RBE estimates by collecting and parameterizing the available *in vitro* data from the literature (Mairani et al. 2016a, Mairani et al. 2016b). Additionally, a mechanism-inspired model called the Repair-Misrepair-Fixation (RMF) model is implemeted for research purposes (Kamp et al. 2014, Kamp et al. 2014, Kamp et al. 2014).

Prior the first patient treatment with helium ions, an RBE model must be selected, integrated into the clinical TPS and extensively validated. This first requires an evaluation of RBE models in their current state and their ability to predict radiation-induced cell death, e.g. for *in vitro* experimentation. Figure 3.4.a depicts RBE model variation for different LET levels and tissue radio-sensitivity factors (α/β_x) as a function of physical dose for four available RBE model for helium ions (LEM, MKM, RMF, DDM). Additionally, *in vitro* data collected for the development of the data-driven RBE model (DDM) for helium ions is presented in figure 3.4.b. In terms of RBE uncertainty, low (α/β_x) signifies a highly radio-resistant tissue that is of particular interest due to the lack of data and substantial variability between RBE models.

In *Publication D*, the Renca cell line was chosen to examine *in vitro* dose-response for helium ion beams. We set out to verify the significant RBE enhancement observed in the models for dose levels < 4 Gy, a clinically relevant range bearing in mind the typical fractionation size for proton beams of ~2 Gy (RBE) (pathology and treatment scheme dependent). One aspect of RBE modelling for helium worth discussing is the computation and handling of the β (quadratic) component of the LQ model. For large Z particles, the β component is often negligible within the typical fractionated dose range and in most conditions. For lower Z particles, however, R_β may exhibit LET-dependent trends more complex than currently understood. It is therefore important to understand R_β for both the primary beam of light ions and mixed field radiation of heavy ion beams (e.g. modeling effective dose nuclear interactions and fragmentation by-products). Close examination of the R_β component of the DDM model (Mairani et al. 2016a, Mairani et al. 2016b) reveals that for LET of ~4 keV μm^{-1}, R_β converges to ~0.6, while for ~15 keV μm^{-1}, R_β approaches ~1. R_β parameterization was obtained by a convenient parameterization which fits the running averages of the experimental data, neglecting any $(\alpha/\beta)_x$ dependencies due to the large uncertainties effecting the β term. Recent works develop a phenomenological model for proton beams from *in vitro* data following a similar approach to R_β handling by assuming a negligible $(\alpha/\beta)_x$ dependency (Mairani et al. 2017b, McNamara et al. 2015). Here, parameter fittings are merged to a relatively small amount of data using a running average and thus, this work can shed light on RBE model performance in regions where data is sparse and predictions exhibit large uncertainties. Moreover, existing experimental data is especially scarce for low $(\alpha/\beta)_x$ values (< 3 Gy) (Mairani et al. 2016b), where the largest RBE values are expected and

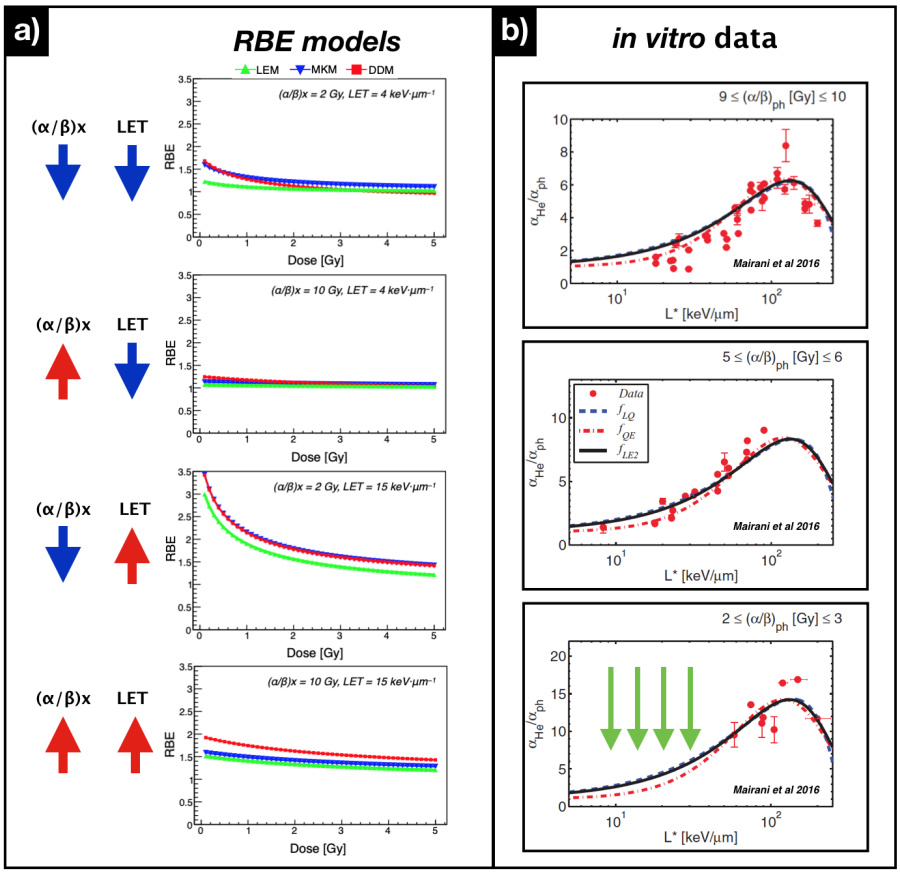

Figure 3.4 – a) RBE model variation for LEM (green), MKM (blue) and DDM (red) as a function of physical dose for different LET levels and tissue radio-sensitivity factors (α/β_x). b) Data collected from *in vitro* clonogenic assay experiments (α_{He}/β_{ph}), organized within three distinct cell line groups: low, moderate and high radio-resistance (from top to bottom). The green arrows draw attention to a region where no data is available within a clinically relevant LET range (between 0 and <50 keV μ m^{-1}. This figure was adapted from Mein et al. and Mairani et al..

the highest variations among the models occur. Further data for low $(\alpha/\beta)_x$ tissues and for clinically-relevant dose levels, especially in standard fractionation regimes (DRBE < ~3 Gy (RBE)), is essential for benchmarking the predictive power of these RBE models. These relatively large uncertainties in R_β fitting for lower LET values (<10 keV μm^{-1}) could be a main source of the disagreement of the models with experimental data, which suggests that further *in vitro* study and tweaking of the models would yield improved RBE predictions with the DDM. The biophysical models would require refinement of their corresponding parameters (Mairani et al. 2017a). However, 5% to 10% predictive power for RBE in the target region is expected and acceptable considering the uncertainty of the reference photon sensitivity measurement.

The results in *Publication D* may imply that systematic uncertainties in the predic-

tion of RBE for helium ions for clinical scenarios are not primarily dominated by the choice of the RBE model. But they may more notably be determined by the choice of the *in vitro* dataset used for tuning the RBE model parameters and the approach and methodology used for tuning itself. Similar conclusions might hold also for RBE models for higher Z ion species. Nonetheless, MKM and DDM presented similar predictions across the various endpoints (i.e. dose and $\mathrm{LET_d}$) while LEM-IV consistently underestimates dose-response for the lower LET conditions.

Additional systematic RBE uncertainties arise from differences between *in vivo* and *in vitro* data. However, due to its scarcity, in vivo and clinical data are hardly used to tune RBE models, but rather for validation of commonly established RBE models (Saager et al. 2015), exception being the neutron-equivalent scaling point used for carbon ions (59,60). Previous works also propose application of clinical data for RBE model tuning in addition to *in vitro* and *in vivo* measurements (Cometto et al. 2014).

Publication D is by no means a complete evaluation of RBE prediction for helium ions. Ongoing works will continue to investigate performance with additional cell lines with a wide range of $(\alpha/\beta)_x$ values as conducted more extensively for proton beams (Chaudhary et al. 2014, Matsumoto et al. 2014, Howard et al. 2017, Guan et al. 2015, Beyreuther et al. 2019). In addition, little is understood about the sensitivity of the RBE models to input uncertainties for helium ions (e.g. absolute values of α_x and β_x). Recent works have perform sensitivity studies using biophysical models for carbon ions such as LEM and MKM (Böhlen et al. 2012, Grün et al. 2017, Kamp et al. 2017 Dahle et al. 2018). Aside from comprehensive evaluation of biological effects and modeling for helium ion beams, ongoing efforts will present a full validation of FRoG against dosimetric measurements, Monte Carlo simulation and biological investigations to produce physical dose, $\mathrm{LET_d}$ and RBE-weighted dose for both clinical and experimental modalities in particle therapy.

3.3 Developing novel treatment and imaging techniques for the clinic

The translation of innovative systems for treatment delivery and monitoring can be drawn-out in series of initial testing and integration steps. Despite dedicated research teams for routine clinical support, useful innovation in medicine may never reach common practice without a transparent port to clinicians. With this in mind, FRoG's sandbox environment contains physics models necessary for dose prediction and can foster development and testing of new techniques in particle therapy for treatment delivery, monitoring and evaluation. As detailed in Section 3.2, the HIT administration and clinical directors have set a start date for clinical trials using helium ion beams. With no commercial treatment planning system currently available

on the market, there is an immediate need for systems capable of generating treatment fields, both physical and biological. In the case of commissioning and simple testing, SOBP plan generation in homogeneous targets is a basic but essential feature, with systems like TRiP98 (Krämer et al. 2016), Hyperion (Fuchs et al. 2012, Fuchs et al. 2015) and FRoG (Mein et al. 2018). Since FRoG is maintained in-house, incorporates the latest physics models for helium ion beams (Horst et al. 2019) using the the FLUKA development version (as well as beam-line specific adaptations) and is the sole GPU-accelerated helium dose engine, FRoG is currently the main support tool for research and clinical investigations for helium ion beams. Initial validations works of FRoG against Monte Carlo and measurements were performed for both physical and biological dose computation (Mein et al. 2018, Mein et al. 2019a). These works were an ideal starting point however they only test a limited set of conditions both physical (in terms of field size, dose level, geometry, etc.) and biological (Renca, a/b ~ 2 Gy). For the purpose of developing a first generation of treatment planning systems for helium ion beam therapy, further validation works for FRoG version 1 (2018) are ongoing. Regarding RBE and effective dose computation for helium ion beams, there is no consensus as to which model is most suitable for clinical application. *Publication D* samples a subset of clinical conditions (i.e. tissue type, field attributes, RBE models) and future works should consider a more long-term view for RBE study and model implementation as depicted in Figure 3.5. Understanding RBE for helium ions remains a key issue in proper clinical use and few recent works present initial estimates (Dokic et al. 2016). Despite the scarcity of data, especially for pristine beams within the clinically relevant LET range, the recently introduced data-driven RBE model (Mairani et al. 2016a, Mairani et al. 2016b) in conjunction with mechanistic models (i.e. LEM and MKM) can provide a first prediction for initial studies. The accuracy of these models is dependent on the reliability of the in vitro data used for tuning, and further efforts in understanding RBE for helium ions is recommended, especially when considering recent reviewers which shed light on issues of experimental reproducibility with radio-biological studies (Draeger et al. 2019).

Since the initial release of FRoG, related efforts in the BioPT group have focused on expanding FRoG functionality and dose engine integration into a fully equipped system, known as the PRECISE TPS (PaRticle thErapy using single and Combined Ion optimization StratEgies). At the moment, clinical assignment of particle beams is purely circumstantial and can be dictated by the clinician's preference, e.g. based on prior indication or anecdotal evidence of clinical outcome from prior or ongoing clinical trials. The PRECISE TPS aims to overcome these shortcomings by providing a system which, for each patient, will generate a set of particle therapy treatments based on a limited number of clinical inputs, for various particle species, using both single and combined modalities. Little is understood about the clinical advantages of combining ions and works within the BioPT group are currently underway in this subject matter. Böhlen et al. first proposed reducing uncertainty in effective dose prediction for carbon ion therapy by optimizing constant RBE

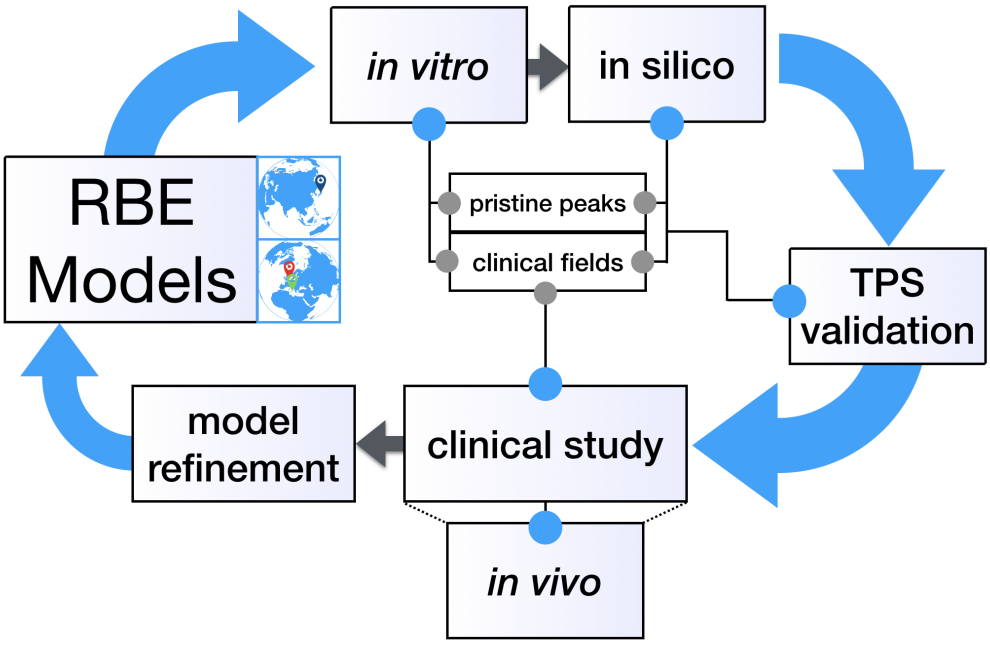

Figure 3.5 – Long-term workflow of helium RBE study and clinical integration of RBE models (biophysical and phenomenological). *In vitro* study and in silico comparisons (using Monte Carlo and analytical methods) for both monoenergetic beams and clinically relevant conditions are underway. After analysis of the predictive power of the RBE model (both intra- and inter-model variability), preparation of clinical routines is possible, beginning with the validation of a clinical TPS, capable of effective dose calculation for helium with the various biological perspectives. With the anticipated clinical boot-up of the helium ion beam therapy program at HIT, clinical studies (i.e. dose escalation) and research-based *in vivo* investigations can lead to RBE model refinement for improved clinical outcome. Clinical practice using RBE models for heavy ions is location dependent i.e. MKM at Japanese centers and LEM mostly at European centers (Italy and Germany).

treatments using multiple ions. Such an approach to optimization can theoretically reduce potential gradients in biological dose prediction, considering uncertainties in treatment planning, such as tissue radio-sensitivity assignment and the applied biological model (Kopp et al. 2019). Similarly, concurrent works ongoing at NIRS present a novel modality called IMPACT (Intensity Modulated comPosite pArtiCle Therapy) (Inaniwa et al. 2017), which aims to expand therapeutic window via optimization of physical dose and LET. Research efforts at GSI focus on overcoming hypoxia-related resistance via so-called "kill-painting" by combining low and high Z to boost LET mid-target in parallel-opposed beam treatments (commonly used for treatment of prostate cancer) (Tinganelli et al. 2015, Sokol et al. 2019).

In regard to treatment monitoring, innovative systems for particle beams such as prompt gamma spectroscopy (Dal Bello et al. 2018, Dal Bello et al. 2019) and ion-

beam radiography (Gehrke et al. 2017, Gehrke et al. 2018b, Gehrke et al. 2018a) have been demonstrated as promising treatment verification techniques for particle therapy and potentially reduce treatment delivery uncertainties by properly locating the BP *in vivo* (Parodi and Polf 2018). Such systems could benefit by integrating with FRoG serving as a bridge between research and clinical environments. Moreover, concurrent works in BioPT in the form of master's theses will establish and evaluate spectral-based stopping power prediction (as opposed to conventional HU-SPR conversion with single energy CT systems) for improved particle range estimation used during treatment planning (Mei et al. 2018, Landry et al. 2019). Similar works investigate clinical viability of advanced dual-energy CT (DECT) systems to mitigate range uncertainties (Bär et al. 2017) and implement into clinical practice (Wohlfahrt et al. 2017). Future aims with FRoG will support and propel such imaging and treatment verification techniques into the clinic.

3.4 Application of FRoG beyond Heidelberg: IBA-based facility

Apart from the initial development, validation and application at the base institutions HIT and CNAO, FRoG can also be used during research and clinical routines at a proton therapy center (PTC), currently the most common form of particle therapy facility (PTCOG 2019). The modern-day PTC administers high-precision cancer treatment using commercial treatment planning and delivery systems to predict patient dose, optimize coverage to deep-seated solid tumors, and minimize risk of adverse effects in nearby healthy tissues. Joining a list of over 50 facilities invested in IBA solutions (Ion Beam Applications SA, Louvain-la-Neuve, Belgium), the Normandy PTC (CYCLHAD) at the Centre François Baclesse (CFB) opened its doors to patients in August 2018, providing proton therapy treatments with the IBA single-room Proteus®ONE using the RayStation® TPS (RaySearch, Stockholm, Sweden) (Ion Beam Applications S.A. 2018a). Such cyclotron-based delivery systems operate using continuous selection (as opposed to discrete energies with a synchrotron) and beam characteristics differ between offered treatment room models as well as vendors using similar equipment. Additionally, treatment planning system (TPS) features and specifications can vary in the context of available output, calculation mode (analytical or condensed history Monte Carlo), run-time and accuracy; however, all commercial systems remain in a pre-compiled format throughout clinical use, preventing the development, testing and integration of innovative physical and biophysical models in particle therapy.

Considering these factors, clinical integration and validation of auxiliary systems, which provide both secondary independent dose prediction during routine QA, as well as advanced physical/biophysical parameters such as LET and RBE-weighted dose, is recommended. Regarding RBE for proton beams, a constant value of 1.1 is

accepted and applied as the clinical standard worldwide, as defined by ICRU, despite evidence of variable RBE for protons. For the moment, there is no streamlined solution to extend biophysical dose computation to the particle therapy clinic (e.g. next-generation beam models, LET_d and variable models) for protons. This is a current setback in the field, especially for smaller clinics which lack the resources and man-power to establish a research support team for the clinic. The AAPM Task Group Report (TG) 256 advises proton therapy centers implement dose-weighted LET into clinical decision-making at the very least to avoid unwarranted biological effects in surrounding critical organs (Paganetti et al. 2019). Contrary to conventional photon radiotherapy with nearly half a century of experience, there is no widely accepted practice for verification of clinical performance using independent dose calculation software. In a sense, the enhanced tumour-targeting features of particle therapy beams (inverted depth dose at end-or-range) make delivery susceptible to uncertainty and therefore, robustness remains a key issue in treatment planning to mitigate range uncertainty and biological effects neglected in the clinic. That being said, one must note the importance of supporting the clinical TPS with advanced secondary systems, e.g. analytical or Monte Carlo codes developed and maintained in-house which offer gold-standard accuracy but require substantial physics and programming expertise for time- and hardware-intensive computation. Recently, several works by large research institutions present facility-specific dose engines, most of which involve task parallelization on a GPU for enhanced speed and superior accuracy compared to conventional systems.

Recently, the FRoG system was installed and commissioned at CYCLHAD to provide various treatment perspectives to clinicians, physicists and dosimetrists. This mainly involved adapting dose computation procedures to a cyclotron-based facility (continuous energy selection). Figure 3.6 presents results from the ongoing validation work of FRoG at the Normandy Proton Therapy Center, depicting FRoG dose prediction against the clinical TPS (RayStation® Monte Carlo, RS-MC) and ion chamber measurements. A representative patient case is additionally displayed in Figure 3.7, demonstrating FRoG's excellent agreement with a commercial Monte Carlo dose engine. Additionally, LET_d and effective dose calculated using a variable RBE model (phenomenological) are presented (Mairani et al. 2017b). Recent reviews assemble and analyze fourteen phenomenological RBE models for proton therapy available in the literature, indicating roughly ~10% uncertainty increasing (for clinical fields) towards the SOBP-end (Rorvik et al. 2018). It is therefore paramount to better understand the behavior of these models and which are most applicable for certain anatomical sites and treatment types (e.g. hyper- versus hypofractionation, dose level, field-size, etc.).

Nonetheless, with FRoG as an auxiliary system for advanced dose computation and verification in conjunction with the clinical TPS (RS-MC), physicians and physicists may predict a more reliable "delivered biological dose" to the patient (compared to current clinical standards), especially in challenging clinical cases, as well as

incorporate LET_d into treatment planning and clinical decision-making.

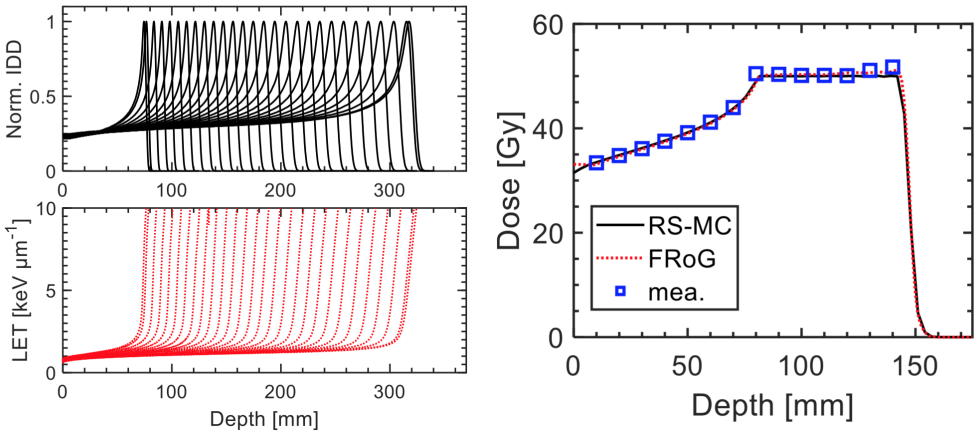

Figure 3.6 – Example FRoG base-data integral depth-dose and depth-LET_d profiles (left) and representative validation test with mid-range depth SOBP profiles (FRoG and RS-MC) against ion chamber measurements (mea.).

At the moment, there is no clear workflow for how to best integrate new metrics like LET_d and variable RBE models into the clinics. Considering the uncertainties in current RBE prediction, choosing a single existing model for clinical implementation may be a bit premature. At the moment, a more practical strategy may involve LET-weighting alongside the conventional RBE of 1.1, e.g. LET_d-based optimization techniques implemented into the clinical TPS at Massachusetts General Hospital (MGH, Boston, Massachusetts, USA). Other major research-based facilities as well as small satellite clinics operate using a clinical TPS without modifications or secondary support systems beyond the status-quo in treatment planning. In the meantime, systems like FRoG are compatible with beam-lines of the major proton therapy vendors (e.g. IBA and Varian) and can provide a training ground for physicians and physicists to begin familiarizing with advanced biophysical endpoints. Here, we offer a case-example for how auxiliary dose engines with LET_d and variable RBE functionality could influence clinical decision-making.

3.5 Future visions for FRoG

The GPU-accelerated aspects of FRoG are saliently attractive features for numerous applications with large data-sets which require lengthy analysis and computation times. Currently in particle therapy, there is a demand for investigations into clinical efficacy and evidence-based practice with particle therapy. Interest is expanding for both photon-based studies as well as inter-particle comparisons.

Interpretation of clinical outcome between facilities may be hindered, especially between the European and Japanese definition of RBE for carbon ions. Recent reports

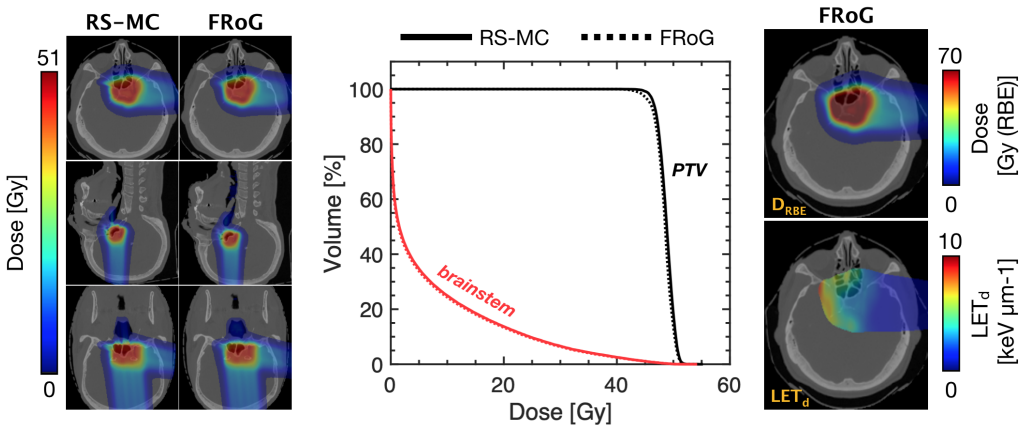

Figure 3.7 – Despite evidence of variable RBE for protons, there is no streamlined solution to access innovative biophysical dose computation. Following recommendations of the AAPM's TG-256, the FRoG platform provides a GPU-accelerated analytical dose engine, capable of LET_d and effective dose computation within minutes, within good agreement of with dosimetric measurements and dose calculated by RayStation Monte Carlo (RS-MC). Dose maps for RS-MC and FRoG are provided (left) for a chordoma patient plan previously treated in Caen, France. Resultant DVH for the PTV and brainstem are provided (middle), along with LET_d and D_{RBE} maps (right).

investigate optic nerve constraints for carbon ions and aim to improve the European RBE-weighted dose (D_{LEM}) constraints by analyzing toxicity in relation to NIRS RBE-weighted dose (D_{MKM}) (Dale et al. 2019). This is of particular importance since carbon ion prescription doses and constraints have mostly been defined and validated within the Japanese biological perspective (Fossati et al. 2012, Fossati et al. 2016, Molinelli et al. 2016). The clinical TPS, for the safety of the patient, have the flexibility to readily change or compute effective dose with various RBE models, and therefore, workarounds using educational or open-source third-party software are useful for understanding clinic outcome (Wieser et al. 2017).

Other examples include FRoG based investigations such as late effect assessment in particle therapy (LEAPt) which are currently underway. Figure 3.8 presents a potential workflow in the LEAPt for analyzing a sub-set of prostate patient treatments, such as the IPI trials (Habl et al. 2016) where 92 patients were treated with either protons or carbon ions. Other recent works assess TCP (Uhl et al. 2014) and NTCP with clinical endpoints for other pathology such as chordoma. FRoG-based investigations will examine clinical outcome against LET_d and variable RBE schemes (i.e. beyond RBE 1.1 for protons and LEM-I effective dose for carbon ions).

In regards to program architecture, there are several projects in the works. In Figure 3.9, FRoG GUI version 2018 (v1.0) is displayed. It's basic user-friendly layout for both clinicians and research scientists yields flexibility and therefore, scripting

features are inherently possible with its open-source architecture written in `python` and `C++` for data-handling and rapid computations, respectively.

At the moment, FRoG functionality is limited to forward calculations; however, broadening FRoG's set of features is currently underway and will be operative within the GUI through sub-commands called *Lily Pads* for both preset and customized subprograms. To name a few, these processes include porting conventionally CPU-based computations to the GPU such as 3D gamma tests, dose calculation and analysis of large patient cohort, physics support for imaging guidance/delivery verification techniques (e.g. prompt γ), advanced biological model development (e.g. based on energy spectra, mechanistic, tumor micro-environment, etc.), multi-modality planning and delivery (i.e. PRECISE) and novel Monte Carlo codes and calculations. Regarding the latter, several Monte Carlo codes were recently made available for protons (Maneval et al. 2019, Jia et al. 2012a, Jia et al. 2012b, Senzacqua et al. 2017, Schiavi et al. 2017). Few works develop fast GPU-based computations for ions heavier than protons (Qin et al. 2017, Qin et al. 2018), which would be particularly valuable considering the introduction of novel particle modalities like raster-scanning helium ion beams and multi-particle treatments. Other reports of an in-house developed TPS using a GPU-based ray-casting analytical engine report optimization and computations under 10 seconds for intensity modulated proton therapy (IMPT) (Matter et al. 2019).

For FRoG, concurrent efforts focus on the development of the various *Lily Pads*. Hybrid approaches (combining analytical and Monte Carlo methods) to dose computation promise compromise between accuracy and calculation speed (Barragán Montero et al. 2018), for example, by scoring heterogeneity index for each ray-trace. If a certain threshold is exceeded, said PB will be flagged for post-processing, and that PB will be pushed to separately calculated using GPU-based Monte Carlo methods. Regarding GPU-based dose optimization, further FRoG developments are currently underway in the PRECISE TPS for single and combined ion-beam treatments. Moreover, as previously mentioned, although $\mathrm{LET_d}$ has been demonstrated as a poor indicator for RBE, one may choose to perform $\mathrm{LET_d}$-optimization to reduce high-LET regions in distal OARs (Unkelbach et al. 2016, Unkelbach and Paganetti 2018). Such techniques will be implemented in FRoG and thoroughly investigated in the near future.

This is only a brief examination and sampling of the aims envisioned for FRoG. The FRoG project extends partnership offers to other interested facilities. As the role of light and heavy ion therapy in cancer therapy continues to expand, fast (e.g. GPU-accelerated) and accurate systems like FRoG will serve as support tools for both research and clinical investigations.

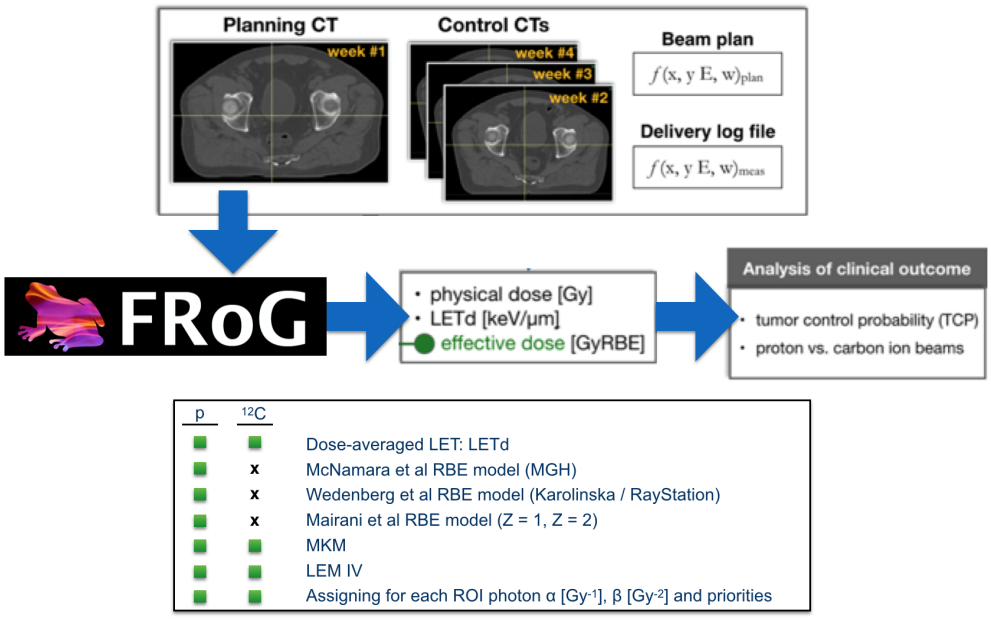

Figure 3.8 – Potential study workflow for analysis of IPI clinical trials. To-date, HIT has treated nearly 400 patients with either protons or carbon ion beams to combat prostate-related disease. Since then, several treatment regimens were applied differing in fractionation scheme and tissue radio-sensitivity factor (α/β_x), used in the local effect model (LEM) during biological dose optimization for carbon ion treatments. With nearly a decade of clinical indication, what can we learn about RBE and its impact on treatment outcome? The first HIT prostate patient cohort from the prospective randomized phase 2 clinical trial (Ion Prostate Irradiation, IPI) is collected here to study biological effect in context of tumor control and normal tissue toxicity. The 92 IPI patients received either proton therapy or carbon ion therapy with identical fraction regime and prescription dose in the target, a total dose of 66 GyRBE administered in 20 fractions. Forward calculations including physical dose, $\mathrm{LET_d}$ and $\mathrm{D_{RBE}}$ will be performed with FRoG. For improved prediction of actual delivered dose, computation is performed using the original planning CT as well as weekly control CTs to account for anatomical changes throughout the treatment course. Biophysical uncertainty in prostate cancer treatment planning and delivery will be investigated to assess clinical efficacy of the two particle therapy modalities.

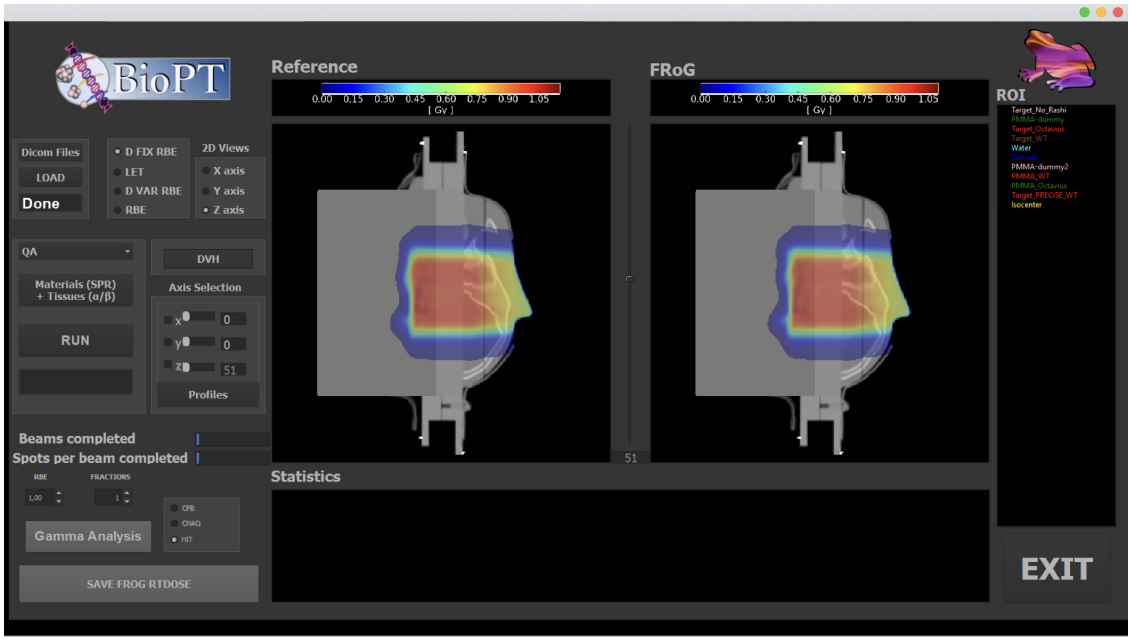

Figure 3.9 – FRoG GUI version 2018.

4 Summary

Radiation therapy is a cornerstone in cancer treatment, with advances stemming from interdisciplinary cooperation between physics, radiation biology and medicine faculties. The emerging field of raster-scanning heavy ion particle therapy was selected among the most promising interdisciplinary explorative fields with high relevance for the “cancer moonshot program". Since the inception of the Heidelberg Ion-beam Therapy (HIT) in 2009, over 5000 patients have been treated with light and heavy ion beams (protons and carbon ions), exploiting its major advantages over the conventional treatment using photons — providing a superior physical dose distribution and increased relative biological effectiveness (RBE) in the tumor region relative to the surrounding healthy tissues.

In this work, a multi-institutional collaboration between HIT (Heidelberg, Germany) and the National Centre of Oncological Hadrontherapy (CNAO, Pavia, Italy), among others, introduces a unique software, FRoG, for rapid and robust dose calculation on a graphics processing unit (GPU) for four ions (p, ^{4}He, ^{12}C and ^{16}O). As opposed to a commercial treatment planning system (TPS) used in the clinic, FRoG is a sandbox environment for radiation therapy research, capable of incorporating both conventional and sophisticated models for physics and biology. Validating against the gold-standard for accuracy (Monte Carlo simulation), we demonstrate the system's potential for upcoming integration in clinical studies.

To best interpret the overall clinical outcome in particle therapy, evaluation and improvement of the predictive biophysical models, derived from *in vitro* studies, in conjunction with physical beam delivery uncertainties remains paramount. This is an important step to compare the strengths and weaknesses of currently established biological models as well as reinforcing development of novel more heuristic approaches. To this end, GPU-based software like FRoG represent a paradigm shift for computation in biomedical research, making complex tasks like big-data analysis commonplace. Deep learning algorithms could now be utilized in conjunction with the 3D dose-distribution calculated by FRoG and imaging based spatially resolved information (radiomics based endpoints) to identify data-driven biological effect oriented dose definition. This is an important step towards the current US National Cancer Institute and German Cancer Research Center (NCI-DKFZ) initiative to define the impact of prescribed dose as a function of biophysical effects.

When it comes to dose calculation accuracy in particle therapy, centers may be reluctant to report common performance issues of the clinical treatment planning system (TPS) in regions of high uncertainty. Present-day dose calculation in the clinic may be knowingly compromised due to range uncertainty and/or limitations in lateral beam modeling near the Bragg peak through beam paths with severe anatomic heterogeneity. Unless clinics perform comprehensive validations in extreme clinical conditions using a robust auxiliary dose calculation method, i.e. independent analytical or Monte Carlo engines, the achievable standards in treatment planning using current practices remain unknown. In this work, we expose the computational limits of various dose calculation systems, for both in-house developed and commercial, used at HIT.

In addition to FRoG, a Monte Carlo-based treatment planning system (MCTP) was developed at HIT for advanced dose calculation and optimization in delicate clinical cases where the gold-standard for accuracy is crucial. Here, these two unique systems are rigorously tested in a worst-case clinical scenario and compared to the current clinical standards of a treatment planning system (TPS) in particle therapy (SyngoPT®, Siemens, Erlangen, Germany). The SyngoPT® TPS was first implemented at HIT in 2008 and is still in use today for light and heavy ion therapy facilities worldwide.

Using multi-dimensional dosimetry, our results indicate that while the advanced in-house systems excelled, clinically relevant discrepancies were observed between measurement and predictions the clinical TPS, shedding light on the limitations of commercial analytical algorithms in treatments with highly inhomogeneous patient anatomy. We provide evidence that both Monte Carlo methods and innovative dose engines (like FRoG) afford considerable improvements in prediction and should become commonplace in particle therapy.

In conjunction with these two clinical particle therapy modalities at HIT, preparations to begin the first raster-scanning helium ion beam therapy program are underway. Currently, helium ions are used solely for experimental studies at HIT, and have remained unexploited worldwide since the shutdown of the clinical trials at the Lawrence Berkeley Laboratory (LBL) in the early 1980's. Their anticipated clinical application will present numerous untapped medical and monetary advantages, considering the superior biophysical properties to protons and the potential for a compact facility design.

Prior to clinical application of helium ions, selection of an appropriate model for relative biological effectiveness (RBE) is essential. In this work, we take the first steps towards evaluating RBE for helium ion beams and three associated models from a clinical standpoint. Inter- and intra-model dependencies were investigated both in silico and subsequently benchmarked *in vitro* . Clinically relevant differences in RBE prediction as a function of the various endpoints (dose, linear energy transfer (LET) and tissue type) were observed. In addition, the models were incorporated

into FRoG which will act as the primary computational tool during the clinical routine as well as during the integration of the first commercial TPS for helium ion therapy.

The cumulative thesis presented here encompasses the four following published works:

A. **Mein S**, Choi K, Kopp B, Tessonnier T, Bauer J, Alfredo F, Haberer T, Debus J, Abdollahi A and Mairani. Fast robust dose calculation on GPU for high-precision ^{1}H, ^{4}He, ^{12}C and ^{16}O ion therapy: the FRoG platform. *Sci. Rep.*, 2018.

B. Choi K, **Mein S**,, Kopp B, Magro G, Molinelli S, Ciocca M and Mairani A. FRoG—A New Calculation Engine for Clinical Investigations with Proton and Carbon Ion Beams at CNAO. *Cancers*, 2018.

C. **Mein S**, Kopp B, Tessonnier T, Ackermann B, Ecker S, Bauer J, Choi K, Aricò G, Ferrari A, Haberer T, Debus J, Abdollahi A and Mairani A. Dosimetric validation of Monte Carlo and analytical dose engines with raster-scanning ^{1}H, ^{4}He, ^{12}C and ^{16}O ion-beams using an anthropomorphic phantom. *Phys. Med.*, 2019.

D. **Mein S**, Dokic I, Klein C, Tessonnier T, Böhlen T T, Magro G, Bauer J, Ferrari A, Parodi K, Haberer T, Debus J, Abdollahi A and Mairani A 2019a Biophysical modeling and experimental validation of relative biological effectiveness (RBE) for 4He ion beam therapy. *Radiat. Oncol.*, 2019.

Publication A details the methods, developmental process and validation of the FRoG physical dose engine at HIT for clinical (p, ^{12}C) and experimental beams (^{4}He and ^{16}O). *Publication B* details dosimetric validations (for p and ^{12}C) and clinical investigations with FRoG as well as $\mathrm{LET_d}$ and effective dose with variable RBE models for carbon ions. *Publication C* investigates the limits of particle therapy dose engines in an anthropomorphic phantom dosimetric study. *Publication D* investigates RBE prediction for helium ion beam therapy and establishes effective dose computations with full Monte Carlo and GPU-accelerated analytical algorithms.

FRoG was recently introduced into the clinical and research pipeline at the National Centre for Oncological Hadrontherapy (CNAO, Pavia, Italy) and is currently under installation for clinical activity at the Danish Center for Particle Therapy (DCPT, Aarhus, Denmark), and the Normandy Proton Therapy Center (Caen, France), with other facility partnerships planned or pending. The extension of FRoG beyond Heidelberg and further applications are explored.

5 Appendix

Dose calculation in heterogeneous settings requires physics knowledge of how particle beams interact in heterogeneous media and how complex anatomy or geometries distort a pristine pencil beam (PB). Monte Carlo simulation inherently accounts for this through particle-by-particle iteration. However, basic analytical algorithms such as the pencil beam model will impose Bragg peak (BP) as a function of depth and spread dose lateral based on an parameterized model, ignoring effects of lateral heterogeneity on the incident beam. The depth wise alterations in density, as long as the incident beam is along the central axis and the geometry is uniform in the tangential plane, will be accounted for in the initial ray-tracing as a range shift. However, lateral variations will distort the PB shape. Therefore, it is essential that analytical algorithms compensate for such effect of lateral heterogeneity on PB pristiness. There are several approaches including ray-casting, WEPL-to water-equivalent path length to point of interest (WEPL-to-POI), and pencil beam splitting. Two main approaches have been implemented in FRoG, both using a pencil beam splitting approach, and will be summarized in the following sections. The goal of pencil beam decomposition is to reconstruct the original distribution with a particular spatial arrangement of scaled sub-Gaussian (normal) distribution, which becomes a unique PB during ray-tracing and computation of lateral dose evolution. This technique becomes of particular use when heterogeneities are introduced into the geometry as demonstrate by Figure 5.1, with PB imaging on a split medium geometry.

All solutions must begin by recalling the definition of a Gaussian function ($G(x)$), a common continuous probability distribution used in many facets of science:

$$G_{\mu,\sigma}(x) = \frac{1}{\sigma} N \left(\frac{x-\mu}{\sigma} \right) \tag{5.1}$$

where μ, σ and N presented the off-set, standard deviation of the Gaussian and normalization factor N, respectively.

1) Dynamic splitting of Gaussian pencil beams

Methods of lateral heterogeneity handling date back to the 1990's , where Schaffner et al. present a fluence-dose model (FDM) approach where each scanned pencil

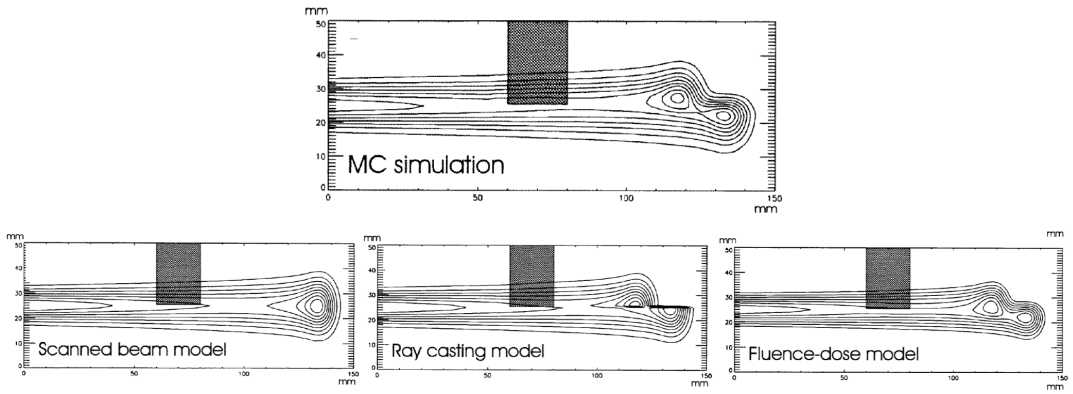

Figure 5.1 – Effect of inhomogeneous geometry (simple two slab system) on PB shape. The "ground truth" Monte Carlo prediction (top) is presented above three analytical approaches: (from left to right) original PB model, ray-casting and fluence-dose model (Schaffner et al. 1999).

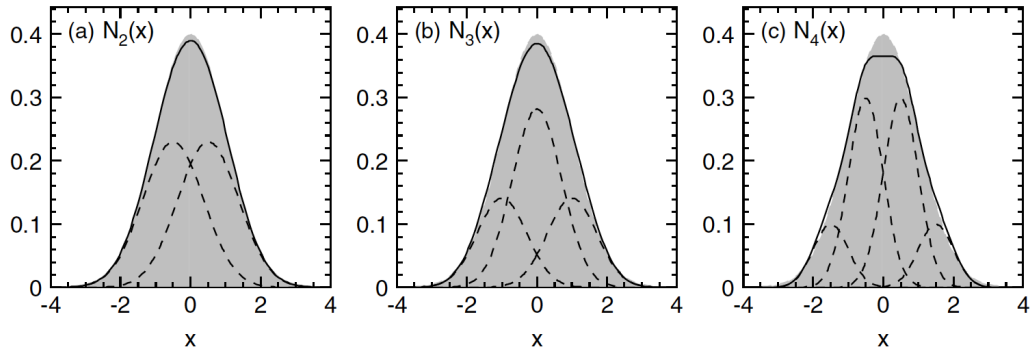

Figure 5.2 – As presented in Kanematsu et al., Lateral profiles of the fixed approximations for the dynamic splitting method. The original normal distribution (highlighted gray region) and approximate solutions (discrete) for reconstruction of order (a) N=2, (b) N=3 and (c) N=4 (solid lines) composed of a subset of sub-Gaussian distributions (dashed lines).

beam is decomposed into elemental PBs, sometimes referred to as daughter PBs and were specifically examined the emerging proton therapy field at the time.

More recent works investigate viable approaches for heavy ions, as detailed in Kanematsu et al. where the authors provide fixed approximate solutions for three unique denominations. in a 2D coordinate system, the original Gaussian distribution can be decomposed with multiplicity M=2, M=3, and M=4, as follows (Fig. 5.2):

$$N_2(x) = \frac{1}{2}\left[G_{-\frac{1}{2},\frac{\sqrt{3}}{2}}(x) + G_{\frac{1}{2},\frac{\sqrt{3}}{2}}(x)\right] \tag{5.2}$$

$$N_3(x) = \frac{1}{4}\left[G_{-1,\frac{1}{\sqrt{2}}}(x) + 2G_{0,\frac{1}{\sqrt{2}}}(x) + G_{1,\frac{1}{\sqrt{2}}}(x)\right] \tag{5.3}$$

$$N_4(x) = \frac{1}{8}\left[G_{-\frac{3}{2},\frac{1}{2}}(x) + 3G_{-\frac{1}{2},\frac{1}{2}}(x) + 3G_{\frac{1}{2},\frac{1}{2}}(x) + G_{\frac{3}{2},\frac{1}{2}}(x)\right] \tag{5.4}$$

The works presented in Kanematsu et al. expands on the mathematical formalism and suggested approach to implementation. The authors makes use of "the self-similar nature of Gaussian distributions" for applications in heavy ion therapy dose calculation (specifically carbon ion beams) which enables the dynamic splitting of Gaussian beams to mimic effects of lateral heterogeneity on PB morphing. From a computational speed standpoint, the dynamic splitting method makes possible fast run-times while moderately accounting for lateral heterogeneity effects. The success of such a techniques is highly dependent on the extent of heterogeneity and quality of the beam-line to transport of particle beam with lateral spread characteristics similar to a single Gaussian. Considering the complexity of the HIT beam-line, FRoG results, which implemented the dynamic splitting approach were sufficient in patients with moderate heterogeneity for heavy ions (^{12}C and ^{16}O). For the lighter ions and cases with severe heterogeneity, the dynamic splitting method was below satisfactory when compared to Monte Carlo predictions. Therefore, the following section explores higher order approximations to Gaussian decomposition.

2) Beamlet superposition approach of Gaussian pencil beams

More recently, works present a novel analytical algorithm for the calculation of scanned ion beams called the the beamlet superposition approach. Again, beginning with the mathematical expression for a Gaussian distribution:

$$G\left(r;\mu_r,\sigma_r\right) = \frac{1}{\sigma_r\sqrt{2\pi}}\exp\left(-\frac{\left(r-\mu_r\right)^2}{2\sigma_r^2}\right) \tag{5.5}$$

which a mean of μ_r and standard deviation σ_r. As stated in Russo et al., $G\left(r;\mu_r,\sigma_r\right)$ can be approximated with a weighted superposition of N sub-Gaussian distributions $g(r;0,\tilde{\sigma_r})$. For the case where $G\left(r;\mu_r,\sigma_r\right)$ is composed of an infinite number of sub-Gaussian components within the bounds of $\pm\infty$, a convolution can be written as:

$$G\left(r;\mu_r,\sigma_r\right) = g\left(r;\mu_r,\hat{\sigma}_r\right) * g\left(r;0,\tilde{\sigma}_r\right) \tag{5.6}$$

where $g\left(r;\mu_r,\hat{\sigma}_r\right)$ represents a weight function with a standard deviation $hat\sigma_r = \sqrt{\sigma_r^2 - \tilde{\sigma}_r^2}$.

For practical purposes in dose calculation in a patient (non-infinite geometry), the Gaussian weight function $g(r;\mu_r,\hat{\sigma}_r)$ can be approximated a set equally spaced

Dirac's delta (increments of δr) between $3.5\hat{\sigma}_r$ and $+3.5\hat{\sigma}_r$. Democratisation of equation 5.6 yields

$$g\left(r;\mu_r,\sigma_r\right) \simeq \sum_{i=-\frac{N-1}{2}}^{+\frac{N-1}{2}} g_{r,i}\, g\left(r;\mu_r + i\Delta r, \tilde{\sigma}_r\right) \tag{5.7}$$

Determination of unique weights $g_{r,i}$ for each sub-Gaussian is visually demonstrated in Figure 5.3 by integration of the original Gaussian between the iterative bounds of each centralized Dirac delta, giving the expression

$$g_{r,i} = \int_{\mu_r+\left(i-\frac{1}{2}\right)\Delta r}^{\mu_r+\left(i+\frac{1}{2}\right)\Delta r} g\left(r;\mu_r,\hat{\sigma}_r\right) \mathrm{d}r. \tag{5.8}$$

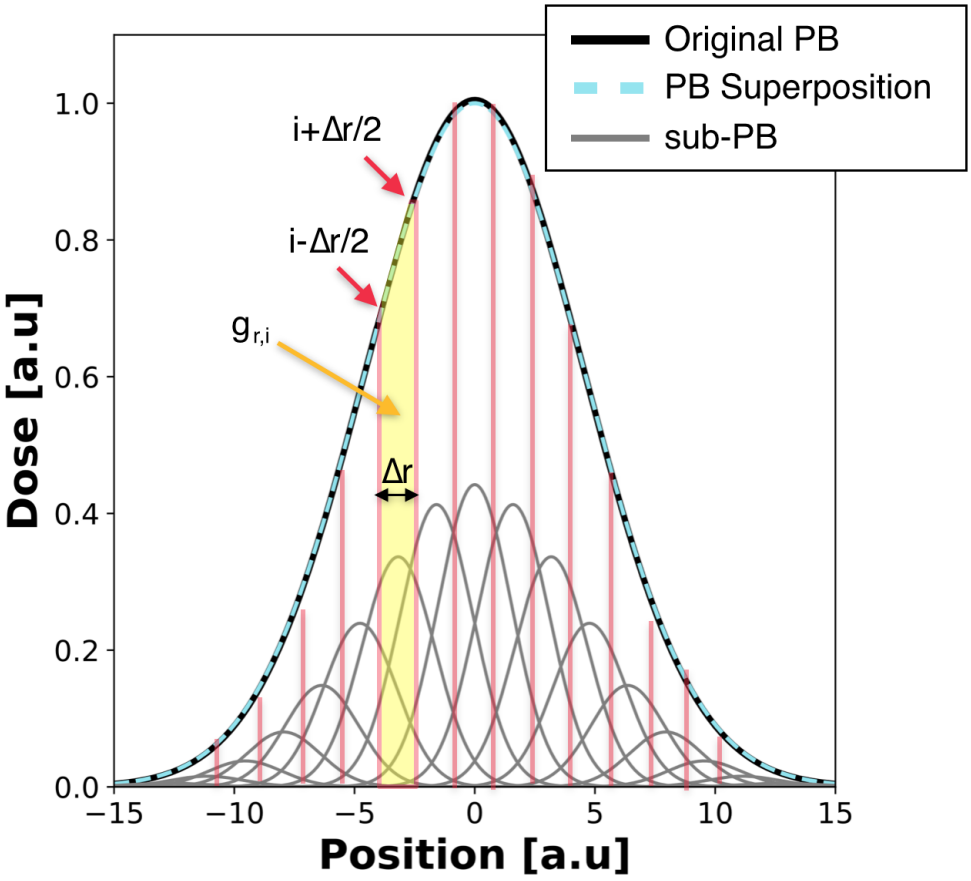

Figure 5.3 – Following the work of Russo et al., 2D representation of beamlet superposition method is presented for an N=21 PB subdivision. The original normal distribution (solid black) and approximate solution (dashed blue) via superposition of an N=21 sub-Gaussian distributions (gray lines).

In FRoG, the beamlet superposition method described above is implemented for raster-scanning proton, helium carbon and oxygen ion beams.

3) Lateral heterogeneity handling in FRoG

FRoG is an analytical dose engine with a Monte Carlo-derived database (both physical and biophysical parameters) and uses a novel approach to the analytical approach, called the dual pencil beam (DPB) model. For lateral heterogeneity handling, high-order pencil-beam subdivision with the beamlet superposition approach described in Russo et al. is applied with a splitting multiplicity of 700 (for p and ^{4}He) and 350 (for ^{12}C and ^{16}O). The source and lateral dose evolution characteristics are described using high-order triple Gaussian (TG) model. Compared to existing commercial systems with analytical dose engines, RayStation, for example, handles anatomic heterogeneity by a hard-coded spatially distributed pencil beam subdivision of 19 (RaySearch). FRoG is the first GPU-based dose engine for (^{4}He, ^{12}C and ^{16}O).

The DPB is established during Monte Carlo simulation of the HIT beam-line for depth dose and lateral dose evolution of the 255 available energies by separately scoring dose contributions from the primary beam particles which interact within the Tungsten wiring of multi-wire proportional chamber (MWPC). This is particularly important for lower Z ions due to relatively significant impact on the pristine beam by inducing large angle scattering, and in turn, an increased low-dose envelope of the impinging particle beam. The effects were not explicitly considered for the higher Z particle beams (^{12}C and ^{16}O).

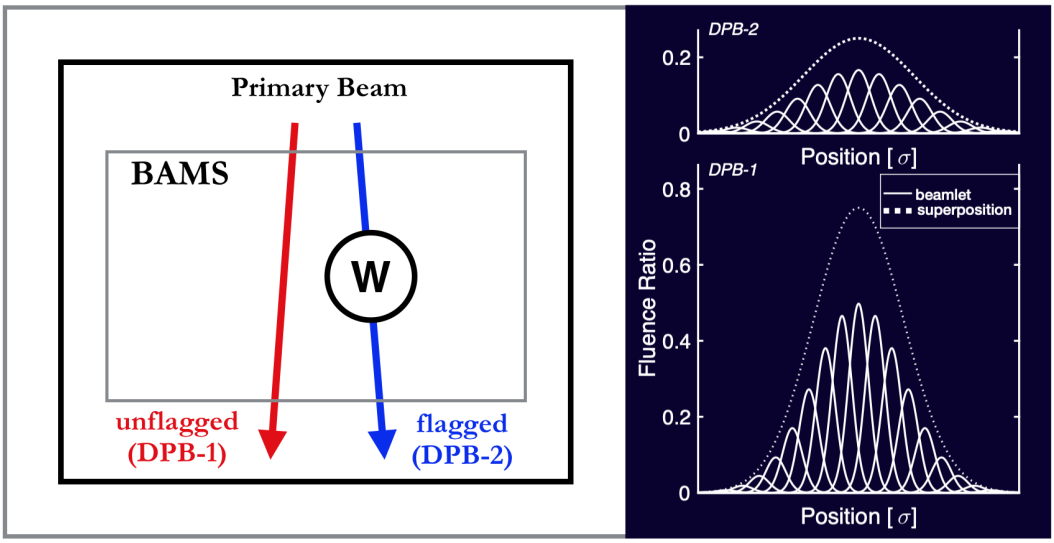

Figure 5.4 – Dual PB (DPB) is implemented in FRoG for p and ^{4}He separately considering primary particles interacting within the Tungsten wiring of MWPC versus the pristine beam (left). Beamlet and beamlet superposition Gaussian for the primary PB (DPB-1, bottom) and the secondary (DPB-2, top) are displayed (right). The superposition (aggregate) of DPB-1 and DPB-2 yield the original primary beam fluence pattern.

Bibliography

Arnold, K. M., Flynn, N. J., Raben, A., Romak, L., Yu, Y., Dicker, A. P., Mourtada, F., & Sims-Mourtada, J. (2018). The Impact of Radiation on the Tumor Microenvironment: Effect of Dose and Fractionation Schedules. *Cancer Growth and Metastasis*. 92

Bär, E., Lalonde, A., Royle, G., Lu, H. M., & Bouchard, H. (2017). The potential of dual-energy CT to reduce proton beam range uncertainties. *Medical Physics*. 100

Barragán Montero, A. M., Souris, K., Sanchez-Parcerisa, D., Sterpin, E., & Lee, J. A. (2018). Performance of a hybrid Monte Carlo-Pencil Beam dose algorithm for proton therapy inverse planning:. *Medical Physics*. 104

Baskar, R., Lee, K. A., Yeo, R., & Yeoh, K. W. (2012). Cancer and radiation therapy: Current advances and future directions. 1

Battistoni, G., Bauer, J., Boehlen, T. T., Cerutti, F., Chin, M. P. W., Dos Santos Augusto, R., Ferrari, A., Ortega, P. G., Kozłowska, W., Magro, G., Mairani, A., Parodi, K., Sala, P. R., Schoofs, P., Tessonnier, T., & Vlachoudis, V. (2016). The FLUKA Code: An Accurate Simulation Tool for Particle Therapy. *Frontiers in Oncology*, 6. 13

Bauer, J., Sommerer, F., Mairani, A., Unholtz, D., Farook, R., Handrack, J., Frey, K., Marcelos, T., Tessonnier, T., Ecker, S., Ackermann, B., Ellerbrock, M., Debus, J., & Parodi, K. (2014). Integration and evaluation of automated Monte Carlo simulations in the clinical practice of scanned proton and carbon ion beam therapy. *Physics in Medicine and Biology*, 59(16):4635–4659. 13

Baumann, M. & Petersen, C. (2005). TCP and NTCP: A basic introduction. 3

Bellinzona, E. V., Ciocca, M., Embriaco, A., Ferrari, A., Fontana, A., Mairani, A., Parodi, K., Rotondi, A., Sala, P., & Tessonnier, T. (2016). A model for the accurate computation of the lateral scattering of protons in water. *Physics in Medicine and Biology*, 61(4):N102–N117. 14

Bentzen, S. M., Constine, L. S., Deasy, J. O., Eisbruch, A., Jackson, A., Marks, L. B., Ten Haken, R. K., & Yorke, E. D. (2010). Quantitative Analyses of Normal Tissue Effects in the Clinic (QUANTEC): An Introduction to the Scientific Issues. *International Journal of Radiation Oncology Biology Physics*. 4

Beyreuther, E., Baumann, M., Enghardt, W., Helmbrecht, S., Karsch, L., Krause, M., Pawelke, J., Schreiner, L., Schürer, M., Von Neubeck, C., & Lühr, A. (2019). Research facility for radiobiological studies at the university proton therapy dresden. *International Journal of Particle Therapy*. 97

Böhlen, T. T., Bauer, J., Dosanjh, M., Ferrari, A., Haberer, T., Parodi, K., Patera, V., & Mairani, A. (2013). A Monte Carlo-based treatment-planning tool for ion beam therapy. *Journal of Radiation Research*, 54(SUPPL.1). 98

Böhlen, T. T., Brons, S., Dosanjh, M., Ferrari, A., Fossati, P., Haberer, T., Patera, V., & Mairani, A. (2012). Investigating the robustness of ion beam therapy treatment plans to uncertainties in biological treatment parameters. *Physics in Medicine and Biology*, 57(23):7983–8004. 97

Böhlen, T. T., Cerutti, F., Chin, M. P. W., Fassò, A., Ferrari, A., Ortega, P. G., Mairani, A., Sala, P. R., Smirnov, G., & Vlachoudis, V. (2014). The FLUKA Code: Developments and challenges for high energy and medical applications. *Nuclear Data Sheets*, 120:211–214. 13

Boyer, A., Biggs, P., Galvin, J., Klein, E., LoSasso, T., Low, D., Mah, K., & Yu, C. (2001). BASIC APPLICATIONS OF MULTILEAF COLLIMATORS. Technical report, AAPM Radiation Therapy Committee Task Group No. 50 Report No. 72. 3

Carabe, A., España, S., Grassberger, C., & Paganetti, H. (2013). Clinical consequences of relative biological effectiveness variations in proton radiotherapy of the prostate, brain and liver. *Physics in Medicine and Biology*. 90

Carabe, A., Moteabbed, M., Depauw, N., Schuemann, J., & Paganetti, H. (2012). Range uncertainty in proton therapy due to variable biological effectiveness. *Physics in Medicine and Biology*. 91

Carabe-Fernandez, A., Dale, R. G., & Jones, B. (2007). The incorporation of the concept of minimum RBE (RBEmin) into the linear-quadratic model and the potential for improved radiobiological analysis of high-LET treatments. *International Journal of Radiation Biology*, 83(1):27–39. 92

Castro, J. R., Char, D. H., Petti, P. L., Daftari, I. K., Quivey, J. M., Singh, R. P., Blakely, E. A., & Phillips, T. L. (1997). 15 years experience with helium ion radiotherapy for uveal melanoma. *International Journal of Radiation Oncology Biology Physics*. 93

Chaudhary, P., Marshall, T. I., Perozziello, F. M., Manti, L., Currell, F. J., Hanton, F., McMahon, S. J., Kavanagh, J. N., Cirrone, G. A. P., Romano, F., Prise, K. M., & Schettino, G. (2014). Relative biological effectiveness variation along monoenergetic and modulated Bragg peaks of a 62-MeV therapeutic proton beam: A preclinical assessment. *International Journal of Radiation Oncology Biology Physics*, 90(1):27–35. 17, 90, 97

Chen, Y. & Ahmad, S. (2012). Empirical model estimation of relative biological effectiveness for proton beam therapy. *Radiation Protection Dosimetry*. 92

Chen, Y., Grassberger, C., Li, J., Hong, T. S., & Paganetti, H. (2018). Impact of potentially variable RBE in liver proton therapy. *Physics in Medicine and Biology*. 91

Chiblak, S., Tang, Z., Lemke, D., Knoll, M., Dokic, I., Warta, R., Moustafa, M., Mier, W., Brons, S., Rapp, C., Muschal, S., Seidel, P., Bendzsus, M., Adeberg, S., Wiestler, O. D., Haberkorn, U., Debus, J., Herold-Mende, C., Wick, W., & Abdollahi, A. (2019). Carbon irradiation overcomes glioma radioresistance by eradicating stem cells and forming an antiangiogenic and immunopermissive niche. *JCI Insight*. 92

Choi, K., Mein, S., Kopp, B., Magro, G., Molinelli, S., Ciocca, M., & Mairani, A. (2018). FRoG—A New Calculation Engine for Clinical Investigations with Proton and Carbon Ion Beams at CNAO. *Cancers*, 10(11):395. 18, 92

Chung, K. (2017). A Pilot Study of the Scanning Beam Quality Assurance Using Machine Log Files in Proton Beam Therapy. *Progress in Medical Physics*. 90

Combs, S. E., Jäkel, O., Haberer, T., & Debus, J. (2010). Particle therapy at the Heidelberg Ion Therapy Center (HIT) - Integrated research-driven university-hospital-based radiation oncology service in Heidelberg, Germany. 18

Cometto, A., Russo, G., Bourhaleb, F., Milian, F. M., Giordanengo, S., Marchetto, F., Cirio, R., & Attili, A. (2014). Direct evaluation of radiobiological parameters from clinical data in the case of ion beam therapy: An alternative approach to the relative biological effectiveness. *Physics in Medicine and Biology*, 59(23):7393–7417. 97

Da Silva, J., Ansorge, R., & Jena, R. (2015). Sub-second pencil beam dose calculation on GPU for adaptive proton therapy. *Physics in Medicine and Biology*, 60(12):4777–4795. 90

Dahle, T. J., Magro, G., Ytre-Hauge, K. S., Stokkevag, C. H., Choi, K., & Mairani, A. (2018). Sensitivity study of the microdosimetric kinetic model parameters for carbon ion radiotherapy. *Physics in Medicine and Biology*. 97

Dal Bello, R., Magalhaes Martins, P., Graça, J., Hermann, G., Kihm, T., & Seco, J. (2019). Results from the experimental evaluation of CeBr3 scintillators for 4He prompt gamma spectroscopy. *Medical Physics*. 99

Dal Bello, R., Magalhaes Martins, P., & Seco, J. (2018). CeBr3 scintillators for 4He prompt gamma spectroscopy: Results from a Monte Carlo optimization study. *Medical Physics*. 99

Dale, J. E., Molinelli, S., Vitolo, V., Vischioni, B., Bonora, M., Magro, G., Pettersen, H. E. S., Mairani, A., Hasegawa, A., Dahl, O., Valvo, F., & Fossati, P. (2019). Optic nerve constraints for carbon ion RT at CNAO – Reporting and relating outcome to European and Japanese RBE. *Radiotherapy and Oncology*. 103

Daniel Bourland, J. (2011). *Radiation Oncology Physics*. 1

Dasu, A. & Toma-Dasu, I. (2013). Impact of variable RBE on proton fractionation. *Medical Physics*. 91

Dokic, I., Mairani, A., Niklas, M., Zimmermann, F., Chaudhri, N., Krunic, D., Tessonnier, T., Ferrari, A., Parodi, K., Jäkel, O., Debus, J., Haberer, T., & Abdollahi, A. (2016). Next generation multi-scale biophysical characterization of high precision cancer particle radiotherapy using clinical proton, helium-, carbon- and oxygen ion beams. *Oncotarget*, 7(35):56676–56689. 93, 98

Draeger, E., Sawant, A., Johnstone, C., Koger, B., Becker, S., Vujaskovic, Z., Jackson, I.-L., & Poirier, Y. (2019). A Dose of Reality: How 20 years of incomplete physics and dosimetry reporting in radiobiology studies may have contributed to the reproducibility crisis. *International Journal of Radiation Oncology*Biology*Physics*. 92, 98

Durante, M. & Loeffler, J. S. (2010). Charged particles in radiation oncology. 2

Durante, M., Orecchia, R., & Loeffler, J. S. (2017). Charged-particle therapy in cancer: Clinical uses and future perspectives. 1

Embriaco, A. (2015). On the parametrization of lateral dose profiles in proton radiation therapy. In: *Proceedings of the 14th International Conference on Nuclear Reaction Mechanisms, NRM 2015*. 14

Embriaco, A., Bellinzona, V. E., Fontana, A., & Rotondi, A. (2017). An accurate model for the computation of the dose of protons in water. *Physica Medica*, 38:66–75. 14, 15

Endo, M. (2018). Robert R. Wilson (1914–2000): the first scientist to propose particle therapy—use of particle beam for cancer treatment. *Radiological Physics and Technology*. 1

Eulitz, J., Lutz, B., Wohlfahrt, P., Dutz, A., Enghardt, W., Karpowitz, C., Krause, M., Troost, E. G. C., & Lühr, A. (2019). A Monte Carlo based radiation response modelling framework to assess variability of clinical RBE in proton therapy. *Physics in Medicine and Biology*. 92

European Organization for Nuclear Research (CERN). FLUKA. 13

Ferrari, A. & others (2005). FLUKA: A multi-particle transport code (Program version 2005). *CERN-2005-010*. 13

Fossati, P., Molinelli, S., Magro, G., Mairani, A., Matsufuji, N., Kanematsu, N., Hasegawa, A., Yamada, S., Kamada, T., Tsujii, H., Ciocca, M., & Orecchia, R. (2016). Carbon ion radiotherapy: do we understand each other? How to compare differentt RBE-weighted dose systems in the clinical setting. *Radiotherapy and Oncology*. 103

Fossati, P., Molinelli, S., Matsufuji, N., Ciocca, M., Mirandola, A., Mairani, A., Mizoe, J., Hasegawa, A., Imai, R., Kamada, T., Orecchia, R., & Tsujii, H. (2012). Dose prescription in carbon ion radiotherapy: A planning study to compare NIRS and LEM approaches with a clinically-oriented strategy. *Physics in Medicine and Biology*, 57(22):7543–7554. 103

Frese, M. C., Wilkens, J. J., Huber, P. E., Jensen, A. D., Oelfke, U., & Taheri-Kadkhoda, Z. (2011). Application of constant vs. variable relative biological effectiveness in treatment planning of intensity-modulated proton therapy. *International Journal of Radiation Oncology Biology Physics*. 92

Fuchs, H., Alber, M., Schreiner, T., & Georg, D. (2015). Implementation of spot scanning dose optimization and dose calculation for helium ions in Hyperion. *Medical Physics*. 94, 98

Fuchs, H., Ströbele, J., Schreiner, T., Hirtl, A., & Georg, D. (2012). A pencil beam algorithm for helium ion beam therapy. *Medical Physics*, 39(11):6726–6737. 94, 98

Fujimoto, R., Kurihara, T., & Nagamine, Y. (2011). GPU-based fast pencil beam algorithm for proton therapy. *Physics in Medicine and Biology*. 90

Garbacz, M., Battistoni, G., Durante, M., Gajewski, J., Krah, N., Patera, V., Rinaldi, I., Schiavi, A., Scifoni, E., Skrzypek, A., Tommasino, F., & Rucinski, A. (2019). Proton therapy treatment plan verification in CCB Krakow using fred Monte Carlo TPS tool. In: *IFMBE Proceedings*. 90

Gehrke, T., Amato, C., Berke, S., & Martišiková, M. (2018a). Theoretical and experimental comparison of proton and helium-beam radiography using silicon pixel detectors. *Physics in Medicine and Biology*. 100

Gehrke, T., Burigo, L., Arico, G., Berke, S., Jakubek, J., Turecek, D., Tessonnier, T., Mairani, A., & Martišíková, M. (2017). Energy deposition measurements of single 1H, 4He and 12C ions of therapeutic energies in a silicon pixel detector. *Journal of Instrumentation*. 100

Gehrke, T., Gallas, R., Jäkel, O., & Martišíková, M. (2018b). Proof of principle of helium-beam radiography using silicon pixel detectors for energy deposition measurement, identification, and tracking of single ions:. *Medical Physics*. 100

Gillmann, C., Jäkel, O., & Karger, C. P. (2019). RBE-weighted doses in target volumes of chordoma and chondrosarcoma patients treated with carbon ion radiotherapy : Comparison of local effect models I and IV. *Radiotherapy and Oncology*, (xxxx):6–10. 18

Giovannini, G., Böhlen, T., Cabal, G., Bauer, J., Tessonnier, T., Frey, K., Debus, J., Mairani, A., & Parodi, K. (2016). Variable RBE in proton therapy: Comparison of different model predictions and their influence on clinical-like scenarios. *Radiation Oncology*, 11(1). 7, 91

Goodhead, D. T. (1994). Initial events in the cellular effects of ionizing radiations: Clustered damage in DNA. *International Journal of Radiation Biology*. 1

Goodhead, D. T. (2006). Energy deposition stochastics and track structure: What about the target? 1

Grün, R., Friedrich, T., Elsässer, T., Krämer, M., Zink, K., Karger, C. P., Durante, M., Engenhart-Cabillic, R., & Scholz, M. (2012). Impact of enhancements in the local effect model (LEM) on the predicted RBE-weighted target dose distribution in carbon ion therapy. *Physics in Medicine and Biology*, 57(22):7261–7274. 93

Grün, R., Friedrich, T., Krämer, M., & Scholz, M. (2017). Systematics of relative biological effectiveness measurements for proton radiation along the spread out Bragg peak: Experimental validation of the local effect model. *Physics in Medicine and Biology*, 62(3):890–908. 97

Guan, F., Bronk, L., Titt, U., Lin, S. H., Mirkovic, D., Kerr, M. S., Zhu, X. R., Dinh, J., Sobieski, M., Stephan, C., Peeler, C. R., Taleei, R., Mohan, R., & Grosshans, D. R. (2015). Spatial mapping of the biologic effectiveness of scanned particle beams: towards biologically optimized particle therapy. *Sci. Rep.*, 5(MAY):9850. 97

Haberer, T., Debus, J., Eickhoff, H., Jäkel, O., Schulz-Ertner, D., & Weber, U. (2004). The heidelberg ion therapy center. *Radiotherapy and Oncology*, 73(0):186–190. 9

Habl, G., Uhl, M., Katayama, S., Kessel, K. A., Hatiboglu, G., Hadaschik, B., Edler, L., Tichy, D., Ellerbrock, M., Haberer, T., Wolf, M. B., Schlemmer, H. P., Debus, J., & Herfarth, K. (2016). Acute Toxicity and Quality of Life in Patients with Prostate Cancer Treated with Protons or Carbon Ions in a Prospective Randomized Phase II Study - The IPI Trial. *International Journal of Radiation Oncology Biology Physics*. 103

Hall, E. J., Astor, M., Bedford, J., Borek, C., Curtis, S. B., Fry, M., Geard, C., Hei, T., Mitchell, J., Oleinick, N., Rubin, J., Ullrich, R., Waldren, C., & Ward, J. (1988). Basic radiobiology. 1

Hawkins, R. B. (1998). A microdosimetric-kinetic theory of the dependence of the RBE for cell death on LET. *Medical Physics*. 9

Hawkins, R. B. (2003). A Microdosimetric-Kinetic Model for the Effect of Non-Poisson Distribution of Lethal Lesions on the Variation of RBE with LET. *Radiation Research*. 9

Hong, L., Goitein, M., Bucciolini, M., Comiskey, R., Gottschalk, B., Rosenthal, S., Serago, C., & Urie, M. (1996). A pencil beam algorithm for proton dose calculations. *Physics in Medicine and Biology*, 41(8):1305–1330. 13, 18

Horst, F., Aricò, G., Brinkmann, K.-T., Brons, S., Ferrari, A., Haberer, T., Mairani, A., Parodi, K., Reidel, C.-A., Weber, U., Zink, K., & Schuy, C. (2019). Measurement of 4He charge- and mass-changing cross sections on H, C, O, and Si targets in the energy range 70–220 MeV/u for radiation transport calculations in ion-beam therapy. *Physical Review C*, 99(1):014603. 94, 98

Howard, M. E., Beltran, C., Anderson, S., Tseung, W. C., Sarkaria, J. N., & Herman, M. G. (2017). Investigating Dependencies of Relative Biological Effectiveness for Proton Therapy in Cancer Cells. *International Journal of Particle Therapy*. 97

Inaniwa, T., Furukawa, T., Kase, Y., Matsufuji, N., Toshito, T., Matsumoto, Y., Furusawa, Y., & Noda, K. (2010). Treatment planning for a scanned carbon beam with a modified microdosimetric kinetic model. *Physics in Medicine and Biology*, 55(22):6721–6737. 9, 93

Inaniwa, T., Furukawa, T., Nagano, A., Sato, S., Saotome, N., Noda, K., & Kanai, T. (2009). Field-size effect of physical doses in carbon-ion scanning using range shifter plates. *Medical Physics*, 36(7):2889–2897. 14, 18

Inaniwa, T., Kanematsu, N., Hara, Y., Furukawa, T., Fukahori, M., Nakao, M., & Shirai, T. (2014). Implementation of a triple Gaussian beam model with subdivision and redefinition against density heterogeneities in treatment planning for scanned carbon-ion radiotherapy. *Physics in Medicine and Biology*, 59(18):5361–5386. 14, 15, 18

Inaniwa, T., Kanematsu, N., Matsufuji, N., Kanai, T., Shirai, T., Noda, K., Tsuji, H., Kamada, T., & Tsujii, H. (2015). Reformulation of a clinical-dose system for carbon-ion radiotherapy treatment planning at the National Institute of Radiological Sciences, Japan. *Physics in Medicine and Biology*, 60(8):3271–3286. 15

Inaniwa, T., Kanematsu, N., Noda, K., & Kamada, T. (2017). Treatment planning of intensity modulated composite particle therapy with dose and linear energy transfer optimization. *Physics in Medicine and Biology*. 99

Ion Beam Applications S.A. (2018a). First patients treated with proton therapy in Caen at the CYCLHAD Center. 100

Ion Beam Applications S.A. (2018b). IBA Dosimetry introduces SciMoCa™, the next-generation Monte Carlo secondary dose check and plan QA solution. 89

Jennings, W. A. (1994). Quantities and units in radiation protection dosimetry. *Nuclear Inst. and Methods in Physics Research, A*. 3

Jia, X., Schümann, J., Paganetti, H., & Jiang, S. B. (2012a). GPU-based fast Monte Carlo dose calculation for proton therapy. *Physics in Medicine and Biology*, 57(23):7783–7797. 18, 90, 104

Jia, X., Schümann, J., Paganetti, H., & Jiang, S. B. (2012b). GPU-based fast Monte Carlo dose calculation for proton therapy. 104

Jia, X., Ziegenhein, P., & Jiang, S. B. (2014). GPU-based high-performance computing for radiation therapy. *Physics in Medicine and Biology*, 59(4):R151–R182. 16, 18

Johnson, J. E., Beltran, C., Wan Chan Tseung, H., Mundy, D. W., Kruse, J. J., Whitaker, T. J., Herman, M. G., & Furutani, K. M. (2019). Highly efficient and sensitive patient-specific quality assurance for spot-scanned proton therapy. *PLoS ONE*. 90

Jones, B., McMahon, S. J., & Prise, K. M. (2018). The Radiobiology of Proton Therapy: Challenges and Opportunities Around Relative Biological Effectiveness. *Clinical Oncology*. 91

Kamp, F., Cabal, G., Mairani, A., Parodi, K., Wilkens, J., & Carlson, D. (2014). Predicting the Relative Biological Effectiveness of Carbon Ion Radiation Therapy Beams Using the Mechanistic Repair-Misrepair-Fixation (RMF) Model and Nuclear Fragment Spectra. *International Journal of Radiation Oncology*Biology*Physics*. 95

Kamp, F., Carlson, D. J., & Wilkens, J. J. (2017). Rapid implementation of the repair-misrepair-fixation (RMF) model facilitating online adaption of radiosensitivity parameters in ion therapy. *Physics in Medicine and Biology*. 97

Kanai, T., Endo, M., Minohara, S., Miyahara, N., Koyama-Ito, H., Tomura, H., Matsufuji, N., Futami, Y., Fukumura, A., Hiraoka, T., Furusawa, Y., Ando, K., Suzuki, M., Soga, F., & Kawachi, K. (1999). Biophysical characteristics of HIMAC clinical irradiation system for heavy-ion radiation therapy. *International Journal of Radiation Oncology Biology Physics*, 44(1):201–210. 9

Kanematsu, N., Komori, M., Yonai, S., & Ishizaki, A. (2009). SU-FF-T-626: Dynamic Splitting of Gaussian Pencil Beams in Heterogeneity-Correction Algorithms for Radiotherapy with Heavy Charged Particles. In: *Medical Physics*, volume 36, page 2669. 16, 112, 113

Knäusl, B., Fuchs, H., Dieckmann, K., & Georg, D. (2016). Can particle beam therapy be improved using helium ions? – A planning study focusing on pediatric patients. *Acta Oncologica*. 94

Kohno, R., Hotta, K., Nishioka, S., Matsubara, K., Tansho, R., & Suzuki, T. (2011). Clinical implementation of a GPU-based simplified Monte Carlo method for a treatment planning system of proton beam therapy. *Physics in Medicine and Biology*. 90

Kooy, H. M., Clasie, B. M., Lu, H. M., Madden, T. M., Bentefour, H., Depauw, N., Adams, J. A., Trofimov, A. V., Demaret, D., Delaney, T. F., & Flanz, J. B. (2010). A Case Study in Proton Pencil-Beam Scanning Delivery. *International Journal of Radiation Oncology Biology Physics*, 76(2):624–630. 18

Kopp, B., Mein, S., Dokic, I., Harrabi, S., Böhlen, T., Haberer, T., Debus, J., Abdollahi, A., & Mairani, A. (2019). Development and validation of single field multi- ion particle therapy treatments. *International Journal of Radiation Oncology*Biology*Physics*, page 69120. 99

Krämer, M. (2009). Swift ions in radiotherapy - Treatment planning with TRiP98. *Nuclear Instruments and Methods in Physics Research, Section B: Beam Interactions with Materials and Atoms*. 10

Kramer, M. & Scholz, M. (2000). Treatment planning for heavy-ion radiotherapy: Calculation and optimization of biologically effective dose. *Physics in Medicine and Biology*, 45(11):3319–3330. 10

Krämer, M., Scifoni, E., Schuy, C., Rovituso, M., Tinganelli, W., Maier, A., Kaderka, R., Kraft-Weyrather, W., Brons, S., Tessonnier, T., Parodi, K., & Durante, M. (2016). Helium ions for radiotherapy? Physical and biological verifications of a novel treatment modality. *Medical Physics*, 43(4):1995–2004. 18, 94, 98

Landry, G., Dörringer, F., Si-Mohamed, S., Douek, P., Abascal, J. F., Peyrin, F., Almeida, I. P., Verhaegen, F., Rinaldi, I., Parodi, K., & Rit, S. (2019). Technical Note: Relative proton stopping power estimation from virtual monoenergetic images reconstructed from dual-layer computed tomography. *Medical Physics*. 100

Lawrence, J. H., Tobias, C. A., Born, J. L., Gottschalk, A., Linfoot, J. A., & Kling, R. P. (1963). Alpha Particle and Proton Beams in Therapy. *JAMA: The Journal of the American Medical Association*. 1

Lawrence, J. H., Tobias, C. A., Linfoot, J. A., Born, J. L., Manougian, E., & Lyman, J. (1965). HEAVY PARTICLES AND THE BRAGG PEAK IN THERAPY. *Annals of internal medicine*. 1

Lee, H. J., Zeng, J., & Rengan, R. (2018). Proton beam therapy and immunotherapy: An emerging partnership for immune activation in non-small cell lung cancer. 2

Li, Y., Tian, Z., Song, T., Wu, Z., Liu, Y., Jiang, S., & Jia, X. (2017). A new approach to integrate GPU-based Monte Carlo simulation into inverse treatment plan optimization for proton therapy. *Physics in Medicine and Biology*. 90

Linstadt, D., Quivey, J. M., Castro, J. R., Andejeski, Y., Phillips, T. L., Hannigan, J., & Gribble, M. (1988). Comparison of helium-ion radiation therapy and split-course megavoltage irradiation for unresectable adenocarcinoma of the pancreas. Final report of a Northern California Oncology Group randomized prospective clinical trial. *Radiology*. 93

Lühr, A., von Neubeck, C., Helmbrecht, S., Baumann, M., Enghardt, W., & Krause, M. (2017). Modeling in vivo relative biological effectiveness in particle therapy for clinically relevant endpoints. *Acta Oncologica*. 92

Lühr, A., von Neubeck, C., Krause, M., & Troost, E. G. (2018). Relative biological effectiveness in proton beam therapy – Current knowledge and future challenges. *Clinical and Translational Radiation Oncology*. 91

Lyman, J. T. & Howard, J. (1977). Dosimetry and instrumentation for helium and heavy ions. *International Journal of Radiation Oncology, Biology, Physics*. 1

Mairani, A., Dokic, I., Magro, G., Tessonnier, T., Bauer, J., Böhlen, T. T., Ciocca, M., Ferrari, A., Sala, P. R., Jäkel, O., Debus, J., Haberer, T., Abdollahi, A., & Parodi, K. (2017a). A phenomenological relative biological effectiveness approach for proton therapy based on an improved description of the mixed radiation field. *Physics in Medicine and Biology*, 62(4):1378–1395. 86, 96

Mairani, A., Dokic, I., Magro, G., Tessonnier, T., Kamp, F., Carlson, D. J., Ciocca, M., Cerutti, F., Sala, P. R., Ferrari, A., Böhlen, T. T., Jäkel, O., Parodi, K., Debus, J., Abdollahi, A., & Haberer, T. (2016a). Biologically optimized helium ion plans: calculation approach and its in vitro validation. *Physics in Medicine and Biology*, 61(11):4283–4299. 93, 94, 95, 96, 98

Mairani, A., Magro, G., Dokic, I., Valle, S. M., Tessonnier, T., Galm, R., Ciocca, M., Parodi, K., Ferrari, A., Jäkel, O., Haberer, T., Pedroni, P., & Böhlen, T. T. (2016b). Data-driven RBE parameterization for helium ion beams. *Physics in Medicine and Biology*, 61(2):888–905. 94, 95, 98

Mairani, A., Magro, G., Tessonnier, T., Böhlen, T. T., Molinelli, S., Ferrari, A., Parodi, K., Debus, J., & Haberer, T. (2017b). Optimizing the modified micro-dosimetric kinetic model input parameters for proton and 4 He ion beam therapy application. *Physics in Medicine and Biology*, 62(11):N244–N256. 85, 92, 93, 95, 101

Maneval, D., Ozell, B. T., & Després, P. (2019). PGPUMCD: An efficient GPU-based Monte Carlo code for accurate proton dose calculations. *Physics in Medicine and Biology*. 90, 104

Marshall, T. I., Chaudhary, P., Michaelidesová, A., Vachelová, J., Davídková, M., Vondráček, V., Schettino, G., & Prise, K. M. (2016). Investigating the Implications of a Variable RBE on Proton Dose Fractionation Across a Clinical Pencil Beam Scanned Spread-Out Bragg Peak. *International Journal of Radiation Oncology Biology Physics*. 91

Matsumoto, Y., Matsuura, T., Wada, M., Egashira, Y., Nishio, T., & Furusawa, Y. (2014). Enhanced radiobiological effects at the distal end of a clinical proton beam: In vitro study. *Journal of Radiation Research*. 97

Matter, M., Nenoff, L., Meier, G., Weber, D. C., Lomax, A. J., & Albertini, F. (2019). Intensity modulated proton therapy plan generation in under ten seconds. *Acta Oncologica*. 90, 104

McMahon, S. J., Paganetti, H., & Prise, K. M. (2018). LET-weighted doses effectively reduce biological variability in proton radiotherapy planning. *Physics in Medicine and Biology*. 91

McNamara, A. L., Schuemann, J., & Paganetti, H. (2015). A phenomenological relative biological effectiveness (RBE) model for proton therapy based on all published in vitro cell survival data. *Physics in Medicine and Biology*, 60(21):8399–8416. 92, 95

Mei, K., Ehn, S., Oechsner, M., Kopp, F. K., Pfeiffer, D., Fingerle, A. A., Pfeiffer, F., Combs, S. E., Wilkens, J. J., Rummeny, E. J., & Noël, P. B. (2018). Dual-layer spectral computed tomography: measuring relative electron density. *European Radiology Experimental*. 100

Mein, S., Choi, K., Kopp, B., Tessonnier, T., Bauer, J., Alfredo, F., Haberer, T., Debus, J., Abdollahi, A., & Mairani, A. (2018). Fast robust dose calculation on GPU for high-precision 1H, 4He, 12C and 16O ion therapy: the FRoG platform. *Sci. Rep.*, page (under review). 18, 90, 98

Mein, S., Dokic, I., Klein, C., Tessonnier, T., Böhlen, T. T., Magro, G., Bauer, J., Ferrari, A., Parodi, K., Haberer, T., Debus, J., Abdollahi, A., & Mairani, A. (2019a). Biophysical modeling and experimental validation of relative biological effectiveness (RBE) for 4He ion beam therapy. *Radiation Oncology*, 14(1):123. 96, 98

Mein, S., Kopp, B., Tessonnier, T., Ackermann, B., Ecker, S., Bauer, J., Choi, K., Aricò, G., Ferrari, A., Haberer, T., Debus, J., Abdollahi, A., & Mairani, A. (2019b). Dosimetric validation of Monte Carlo and analytical dose engines with raster-scanning 1H, 4He, 12C, and 16O ion-beams using an anthropomorphic phantom. *Physica Medica*, 64(March):123–131. 88

Molinelli, S., Magro, G., Mairani, A., Matsufuji, N., Kanematsu, N., Inaniwa, T., Mirandola, A., Russo, S., Mastella, E., Hasegawa, A., Tsuji, H., Yamada, S., Vischioni, B., Vitolo, V., Ferrari, A., Ciocca, M., Kamada, T., Tsujii, H., Orecchia,

R., & Fossati, P. (2016). Dose prescription in carbon ion radiotherapy: How to compare two different RBE-weighted dose calculation systems. *Radiotherapy and Oncology*. 103

Nikjoo, H., Uehara, S., Wilson, W. E., Hoshi, M., & Goodhead, D. T. (1998). Track structure in radiation biology: Theory and applications. In: *International Journal of Radiation Biology*. 6

Oesten, H., Neubeck, C. v., Jakob, A., Enghardt, W., Krause, M., McMahon, S. J., Grassberger, C., Paganetti, H., & Lühr, A. (2019). Predicting In Vitro Cancer Cell Survival Based on Measurable Cell Characteristics. *Radiation Research*. 92

Oiseth, S. J. & Aziz, M. S. (2017). Cancer immunotherapy: a brief review of the history, possibilities, and challenges ahead. *Journal of Cancer Metastasis and Treatment*. 2

Ondreka, D. & Weinrich, U. (2008). The heidelberg ION Therapy (HIT) accelerator coming into operation. In: *EPAC 2008 - Contributions to the Proceedings*. 5

Paganetti, H. (2012). Range uncertainties in proton therapy and the role of Monte Carlo simulations. 11, 90

Paganetti, H., Blakely, E., Carabe-Fernandez, A., Carlson, D. J., Das, I. J., Dong, L., Grosshans, D., Held, K. D., Mohan, R., Moiseenko, V., Niemierko, A., Stewart, R. D., & Willers, H. (2019). Report of the AAPM TG-256 on the relative biological effectiveness of proton beams in radiation therapy. *Medical Physics*. 101

Paganetti, H., Niemierko, A., Ancukiewicz, M., Gerweck, L. E., Goitein, M., Loeffler, J. S., & Suit, H. D. (2002). Relative biological effectiveness (RBE) values for proton beam therapy. *International Journal of Radiation Oncology Biology Physics*. 10, 17, 90

Parodi, K., Mairani, A., Brons, S., Hasch, B. G., Sommerer, F., Naumann, J., Jäkel, O., Haberer, T., & Debus, J. (2012). Monte Carlo simulations to support start-up and treatment planning of scanned proton and carbon ion therapy at a synchrotron-based facility. *Physics in Medicine and Biology*, 57(12):3759–3784. 13

Parodi, K., Mairani, A., & Sommerer, F. (2013). Monte Carlo-based parametrization of the lateral dose spread for clinical treatment planning of scanned proton and carbon ion beams. *Journal of Radiation Research*, 54(SUPPL.1). 14

Parodi, K. & Polf, J. C. (2018). In vivo range verification in particle therapy. In: *Medical Physics*. 100

Peeler, C. R., Mirkovic, D., Titt, U., Blanchard, P., Gunther, J. R., Mahajan, A., Mohan, R., & Grosshans, D. R. (2016). Clinical evidence of variable proton biological effectiveness in pediatric patients treated for ependymoma. *Radiotherapy and Oncology*, 121(3):395–401. 17, 90

PTCOG (2019). https://www.ptcog.ch. 100

Qin, N., Pinto, M., Tian, Z., Dedes, G., Pompos, A., Jiang, S. B., Parodi, K., & Jia, X. (2017). Initial development of goCMC: A GPU-oriented fast cross-platform Monte Carlo engine for carbon ion therapy. *Physics in Medicine and Biology*. 90, 104

Qin, N., Shen, C., Tsai, M. Y., Pinto, M., Tian, Z., Dedes, G., Pompos, A., Jiang, S. B., Parodi, K., & Jia, X. (2018). Full Monte Carlo–Based Biologic Treatment Plan Optimization System for Intensity Modulated Carbon Ion Therapy on Graphics Processing Unit. *International Journal of Radiation Oncology Biology Physics*. 90, 104

Rorvik, E., Fjera, L. F., Dahle, T. J., Dale, J. E., Engeseth, G. M., Stokkevag, C. H., Thörnqvist, S., & Ytre-Hauge, K. S. (2018). Exploration and application of phenomenological RBE models for proton therapy. *Physics in Medicine and Biology*. 9, 92, 101

Russo, G., Attili, A., Battistoni, G., Bertrand, D., Bourhaleb, F., Cappucci, F., Ciocca, M., Mairani, A., Milian, F. M., Molinelli, S., Morone, M. C., Muraro, S., Orts, T., Patera, V., Sala, P., Schmitt, E., Vivaldo, G., & Marchetto, F. (2016). A novel algorithm for the calculation of physical and biological irradiation quantities in scanned ion beam therapy: the beamlet superposition approach. *Physics in Medicine and Biology*, 61(1):183–214. 16, 113, 114, 115

Saager, M., Glowa, C., Peschke, P., Brons, S., Grün, R., Scholz, M., Huber, P. E., Debus, J., & Karger, C. P. (2015). Split dose carbon ion irradiation of the rat spinal cord: Dependence of the relative biological effectiveness on dose and linear energy transfer. *Radiotherapy and Oncology*, 117(2):358–363. 97

Saager, M., Peschke, P., Welzel, T., Huang, L., Brons, S., Grün, R., Scholz, M., Debus, J., & Karger, C. P. (2018). Late normal tissue response in the rat spinal cord after carbon ion irradiation. *Radiation Oncology*. 90, 92

Sánchez-Parcerisa, D., Kondrla, M., Shaindlin, A., & Carabe, A. (2014). FoCa: a modular treatment planning system for proton radiotherapy with research and educational purposes. *Physics in medicine and biology*, 59(23):7341–7360. 18

Sánchez-Parcerisa, D., López-Aguirre, M., Dolcet Llerena, A., & Udías, J. M. (2019). MultiRBE: Treatment planning for protons with selective radiobiological effectiveness. *Medical Physics*. 92

Saunders, W., Castro, J. R., Chen, G. T. Y., Collier, J. M., Zink, S. R., Pitluck, S., Phillips, T. L., Char, D., Gutin, P., Gauger, G., Tobias, C. A., & Alpen, E. L. (2006). Helium-Ion Radiation Therapy at the Lawrence Berkeley Laboratory: Recent Results of a Northern California Oncology Group Clinical Trial. *Radiation Research Supplement*. 93

Scandurra, D., Albertini, F., Van Der Meer, R., Meier, G., Weber, D. C., Bolsi, A., & Lomax, A. (2016). Assessing the quality of proton PBS treatment delivery using machine log files: Comprehensive analysis of clinical treatments delivered at PSI Gantry 2. *Physics in Medicine and Biology*, 61(3):1171–1181. 90

Schaffner, B., Pedroni, E., & Lomax, A. (1999). Dose calculation models for proton treatment planning using a dynamic beam delivery system: An attempt to include density heterogeneity effects in the analytical dose calculation. *Physics in Medicine and Biology*, 44(1):27–41. 111, 112

Schardt, D., Elsässer, T., & Schulz-Ertner, D. (2010). Heavy-ion tumor therapy: Physical and radiobiological benefits. 3

Schiavi, A., Senzacqua, M., Pioli, S., Mairani, A., Magro, G., Molinelli, S., Ciocca, M., Battistoni, G., & Patera, V. (2017). Fred: A GPU-accelerated fast-Monte Carlo code for rapid treatment plan recalculation in ion beam therapy. *Physics in Medicine and Biology*. 90, 104

Scholz, M., Kellerer, A. M., Kraft-Weyrather, W., & Kraft, G. (1997). Computation of cell survival in heavy ion beams for therapy: The model and its approximation. *Radiation and Environmental Biophysics*, 36(1):59–66. 10

Senzacqua, M., Schiavi, A., Patera, V., Pioli, S., Battistoni, G., Ciocca, M., Mairani, A., Magro, G., & Molinelli, S. (2017). A fast - Monte Carlo toolkit on GPU for treatment plan dose recalculation in proton therapy. In: *Journal of Physics: Conference Series*. 104

Shen, J., Liu, W., Stoker, J., Ding, X., Anand, A., Hu, Y., Herman, M. G., & Bues, M. (2016). An efficient method to determine double Gaussian fluence parameters in the eclipse™ proton pencil beam model. *Medical Physics*. 14

Siddon, R. L. (1985). Prism representation: A 3D ray-tracing algorithm for radiotherapy applications. *Physics in Medicine and Biology*, 30(8):817–824. 18

Sokol, O., Krämer, M., Durante, M., Scifoni, E., & Hild, S. (2019). Kill painting of hypoxic tumors with multiple ion beams. *Physics in Medicine & Biology*. 99

Sørensen, B. S., Overgaard, J., & Bassler, N. (2011). In vitro RBE-LET dependence for multiple particle types. 90

Ströbele, J., Schreiner, T., Fuchs, H., & Georg, D. (2012). Comparison of basic features of proton and helium ion pencil beams in water using GATE. *Zeitschrift fur Medizinische Physik*, 22(3):170–178. 94

Tessonnier, T. (2017). *Treatment of low-grade meningiomas with protons and helium ions*. PhD thesis, Ludwig Maximilian University of Munich. 94

Tessonnier, T., Böhlen, T. T., Ceruti, F., Ferrari, A., Sala, P., Brons, S., Haberer, T., Debus, J., Parodi, K., & Mairani, A. (2017a). Dosimetric verification in water of a Monte Carlo treatment planning tool for proton, helium, carbon and oxygen ion beams at the Heidelberg Ion Beam Therapy Center. *Physics in Medicine and Biology*, 62(16):6579–6594. 94

Tessonnier, T., Mairani, A., Brons, S., Haberer, T., Debus, J., & Parodi, K. (2017b). Experimental dosimetric comparison of 1H, 4He, 12C and 16O scanned ion beams. *Physics in Medicine and Biology*. 94

Tessonnier, T., Mairani, A., Brons, S., Sala, P., Cerutti, F., Ferrari, A., Haberer, T., Debus, J., & Parodi, K. (2017c). Helium ions at the heidelberg ion beam therapy center: Comparisons between FLUKA Monte Carlo code predictions and dosimetric measurements. *Physics in Medicine and Biology*, 62(16):6784–6803. 93, 94

Tessonnier, T., Mairani, A., Chen, W., Sala, P., Cerutti, F., Ferrari, A., Haberer, T., Debus, J., & Parodi, K. (2018). Proton and Helium Ion Radiotherapy for Meningioma Tumors: A Monte Carlo-based Treatment Planning Comparison. *Radiation Oncology*, 13(1). 94

Tessonnier, T., Marcelos, T., Mairani, A., Brons, S., & Parodi, K. (2016). Phase Space Generation for Proton and Carbon Ion Beams for External Users' Applications at the Heidelberg Ion Therapy Center. *Frontiers in Oncology*, 5. 13

Tinganelli, W., Durante, M., Hirayama, R., Krämer, M., Maier, A., Kraft-Weyrather, W., Furusawa, Y., Friedrich, T., & Scifoni, E. (2015). Kill-painting of hypoxic tumours in charged particle therapy. *Scientific Reports*. 99

Uhl, M., Mattke, M., Welzel, T., Roeder, F., Oelmann, J., Habl, G., Jensen, A., Ellerbrock, M., Jäkel, O., Haberer, T., Herfarth, K., & Debus, J. (2014). Highly effective treatment of skull base chordoma with carbon ion irradiation using a raster scan technique in 155 patients: First long-term results. *Cancer*, 120(21):3410–3417. 103

Unkelbach, J., Botas, P., Giantsoudi, D., Gorissen, B. L., & Paganetti, H. (2016). Reoptimization of Intensity Modulated Proton Therapy Plans Based on Linear Energy Transfer. *International Journal of Radiation Oncology Biology Physics*. 91, 92, 104

Unkelbach, J. & Paganetti, H. (2018). Robust Proton Treatment Planning: Physical and Biological Optimization. 91, 104

Valdes, G., Chan, M. F., Lim, S. B., Scheuermann, R., Deasy, J. O., & Solberg, T. D. (2017). IMRT QA using machine learning: A multi-institutional validation. *Journal of Applied Clinical Medical Physics*. 89

Valdes, G., Scheuermann, R., Hung, C. Y., Olszanski, A., Bellerive, M., & Solberg, T. D. (2016). A mathematical framework for virtual IMRT QA using machine learning. *Medical Physics*. 89

Wan Chan Tseung, H. S., Ma, J., Kreofsky, C. R., Ma, D. J., & Beltran, C. (2016). Clinically Applicable Monte Carlo–based Biological Dose Optimization for the Treatment of Head and Neck Cancers With Spot-Scanning Proton Therapy. *International Journal of Radiation Oncology Biology Physics*. 90

Wang, Q., Schlegel, N., Moyers, M., Lin, J., Hong, L., Chen, H., Johnson, A., Li, J., Shen, Z., Xu, M., Taddei, P. J., & Yepes, P. (2018). Validation of the fast dose calculator for Shanghai Proton and Heavy Ion Center. *Biomedical Physics and Engineering Express*. 90

Wedenberg, M., Lind, B. K., & Hårdemark, B. (2013). A model for the relative biological effectiveness of protons: The tissue specific parameter α/β of photons is a predictor for the sensitivity to LET changes. *Acta Oncologica*, 52(3):580–588. 92

Wieser, H. P., Cisternas, E., Wahl, N., Ulrich, S., Stadler, A., Mescher, H., Muller, L. R., Klinge, T., Gabrys, H., Burigo, L., Mairani, A., Ecker, S., Ackermann, B., Ellerbrock, M., Parodi, K., Jakel, O., & Bangert, M. (2017). Development of the open-source dose calculation and optimization toolkit matRad. *Medical Physics*, 44(6):2556–2568. 18, 103

Wilkens, J. J. & Oelfke, U. (2004). A phenomenological model for the relative biological effectiveness in therapeutic proton beams. *Physics in Medicine and Biology*, 49(13):2811–2825. 92

Willers, H., Allen, A., Grosshans, D., McMahon, S. J., von Neubeck, C., Wiese, C., & Vikram, B. (2018). Toward A variable RBE for proton beam therapy. 92

Wilson, R. R. (1946). Radiological use of fast protons. *Radiology*. 1

Wohlfahrt, P., Möhler, C., Hietschold, V., Menkel, S., Greilich, S., Krause, M., Baumann, M., Enghardt, W., & Richter, C. (2017). Clinical Implementation of Dual-energy CT for Proton Treatment Planning on Pseudo-monoenergetic CT scans. *International Journal of Radiation Oncology Biology Physics*. 100

Yepes, P. P., Mirkovic, D., & Taddei, P. J. (2010). A GPU implementation of a track-repeating algorithm for proton radiotherapy dose calculations. *Physics in Medicine and Biology*. 90

Zhu, X. R., Li, Y., Mackin, D., Li, H., Poenisch, F., Lee, A. K., Mahajan, A., Frank, S. J., Gillin, M. T., Sahoo, N., & Zhang, X. (2015). Towards effective and efficient patient-specific quality assurance for spot scanning proton therapy. 90

Acknowledgements

I must start this acknowledgement by thanking **PD Dr. Andrea Mairani** for inviting me to Heidelberg for the PhD thesis. The last three years have been highly rewarding both professionally and personally. You were an exceptional adviser. Thank you for the motivation both at work and outside of HIT with occasional running/swimming sessions. I'm looking forward to the next steps for the BioPT group.

I thank my supervisors **Dr. Dr. Amir Abdollahi** and **Prof. Dr. Dr. Jürgen Debus** for providing resources within the Translational Radiation Oncology Group (E210), supporting me at DKFZ-TAC meetings and advising at the physics department. Additionally, I thank Prof. Dr. Dr. Jürgen Debus and **Prof. Dr. Oliver Jäkel** for agreeing to act as referees for this thesis. I would also like to greatly thank my radiobiology supervisor, **Dr. Ivana Dokic**.

My first year of PhD at HIT was highly productive largely in part to the supervision from **Dr. Thomas Tessonnier**. Thank you for being an awesome mentor and friend. I'm excited to hear about your next professional endeavours.

The success of this project cannot be stated without crediting the close collaboration of the FRoG team. A very special thanks to **Benedikt Kopp** and **Kungdon Choi**. I also acknowledge other group members and office-mates such as **Dr. Julia Bauer**, **Judith Besuglow**, **Friderike Faller**, **Carmen Klein**, **Hans Liew** and **Claudia Rittermüller**.

I would like to thank the HIT scientific director **Prof. Dr. Thomas Haberer** for his support during the PhD and in various aspects of the FRoG project. Moreover, I thank **Dr. Semi Harrabi**, **Swantje Ecker** and **Benjamin Ackermann**, who were especially helpful in relations with the clinical team.

I'd also like to acknowledge my previous mentors from the US, **Dr. Leith Rankine** and **Dr. Titania Juang**. The MRIgRT work was really rewarding and this served as a solid foundation for the PhD. Thanks for your support during this time and hope we meet at the next AAPM.

To **Natasha Anstee**, **Vincent Carpenter**, **Mariana Coelho**, **Riccardo Dal Bello**, **Megan Druce**, **Mattia Falcone**, **Marie Groth**, **Julius Gräsel**, **Jacob Isbell**, **Diana Kossakowska**, **Lukas Pilz**, **Manuel Reitbereger**, **Sina Stäble**

and **Franzy Zickgraf**: You are all awesome. Thank you for the support during this time. I wish you all the best with the next steps during and after PhD/Post-doc.

Julius Kaiser: We had a great neighborhood the past three years. Thank you for the support and I wish you the best with your new position in Munich.

Michael Cox, **Rachael Hachadorian**, **Sanjay Hariharan**, **Rudra Pampati**, **Anita Saggurti**, **Turner Reshetar**, **Tyler Wallach**: Thanks for staying in touch while I've been abroad.

Adam El Sehamy: Despite the time zone difference, we managed to become better friends. Thank you for supporting me through visits, travels and hang outs with **Alex El Sehamy**, **Amanda Simone**, **Zhibo Wang** and **Jonas Quill**.

Most importantly, I want to thank my parents, **Laura Galbraith** and **Stewart Beideman Mein III**, and sister, **Hannah Mein**. Thank you for supporting me with everything I do. I am fortunate and hope you are proud of this work.

Erklärung

Ich erkläre hiermit, dass ich die vorgelegte Dissertation selbst verfasst und mich dabei keiner anderen, als der von mir ausdrücklich bezeichneten Quellen und Hilfen bedient habe.

Heidelberg, den Datum

.....